

# Redox-Induced Indenyl Slippage in $[\text{IndCpMoL}_2]^{2+/+/-0}$ Complexes

Carla A. Gamelas,<sup>†,‡</sup> Eberhardt Herdtweck,<sup>§</sup> João P. Lopes,<sup>†</sup> and Carlos C. Romão<sup>\*,†</sup>

*Instituto de Tecnologia Química e Biológica da Universidade Nova de Lisboa, Quinta do Marquês, EAN, Apt 127, 2781-901 Oeiras, Portugal, Escola Superior de Tecnologia, Instituto Politécnico de Setúbal, 2900 Setúbal, Portugal, and Anorganisch-chemisches Institut, Technische Universität München, D-85478 Garching, Federal Republic of Germany*

Received October 6, 1998

The dicationic complexes  $[\text{IndCpMoL}_2]^{2+}$  (Ind = indenyl; Cp = cyclopentadienyl; **1**,  $\text{L}_2 = \text{dppe}$ ; **2**,  $\text{L} = \text{PMe}_3$ ; **4**,  $\text{L}_2 = \text{Bipy}$ ; **5**,  $\text{L}_2 = {}^t\text{Bu}_2\text{bipy}$ ; **6**,  $\text{L}_2 = \text{H}_2\text{biim}$ ; **7**,  $\text{L} = \text{CO}$  and  $\text{CNMe}$ ; **8**,  $\text{L} = \text{CNMe}$ ; **9**,  $\text{L} = \text{CN}^t\text{Bu}$ ; **10**,  $\text{L} = \text{NCMe}$  and  $\text{NMF}$ ; **11**,  $\text{L} = \text{NMF}$ ) were synthesized from  $[\text{IndCpMoL}'_2]^{2+}$  ( $\text{L}' = \text{CO}$ ,  $\text{NCMe}$ ),  $[\text{IndCpMo}(\text{NCMe})\text{Cl}]\text{BF}_4$ , or  $\text{IndCpMoCl}_2$  by ligand substitution. The neutral complexes  $(\eta^3\text{-Ind})\text{CpMoL}_2$  (**13**,  $\text{L}_2 = \text{dppe}$ ; **14**,  $\text{L} = \text{PMe}_3$ ; **15**,  $\text{L}_2 = \text{Bipy}$ ; **16**,  $\text{L} = \text{CO}$  and  $\text{CNMe}$ ; **17**,  $\text{L} = \text{CN}^t\text{Bu}$ ) were obtained upon reduction of the respective dications with  $\text{Cp}_2\text{Co}$ .  $(\eta^3\text{-Ind})\text{CpMo}(\text{dppe})$  (**13**) was also prepared by deprotonation of the cyclopentadiene cation  $[\text{IndMo}(\eta^4\text{-C}_5\text{H}_6)(\text{dppe})]\text{BF}_4$  (**12**) with  $\text{NEt}_3$ . The cyclic voltammograms of the dications present one reversible 2e reduction step from Mo(IV) to Mo(II) except for **1**, **2**, and **6**, in which cases two reversible 1e waves are observed. The ring-slipped complexes  $(\eta^3\text{-Ind})\text{CpMoL}_2$  and the parent dications present similar CV's. The X-ray crystal structures of  $[\text{IndCpModppe}][\text{BF}_4]_2$  and  $(\eta^3\text{-Ind})\text{CpMo}(\text{dppe})$  confirm the indenyl ring planar  $\eta^5$  coordination and slip-folded  $\eta^3$ , respectively.

## Introduction

Ring slippage is a response of a coordinated polyenyl group to the changes in the electron count at the metal center. These changes are usually caused by the addition of two-electron ligands to the metal, as in ligand substitution associative reactions, but may also arise from redox processes. This latter aspect was first experimentally established by Fischer and Elschenbroich, who showed that the 2e reduction of the 18e dication  $[\text{Ru}(\eta^6\text{-C}_6\text{Me}_6)_2]^{2+}$  with Na produces the neutral complex  $\text{Ru}(\eta^6\text{-C}_6\text{Me}_6)(\eta^4\text{-C}_6\text{Me}_6)$ .<sup>1</sup> The bending of the benzene ring in the  $\eta^4$  coordination was confirmed by X-ray studies.<sup>2</sup> Such ring slippages may also be induced electrochemically, as shown in greater detail by the groups of Boekelheide<sup>3</sup> and Geiger<sup>4</sup> for the case of the  $[\text{Ru}(\eta\text{-arene})_2]^{2+/+/-0}$  system, as well as by Weaver<sup>5</sup> and Geiger for the isoelectronic group 9 congeners  $[\text{MCp}^*(\eta^6\text{-arene})]^{2+/+/-0}$  ( $\text{M} = \text{Co}$ ,  $\text{Rh}$ ,  $\text{Ir}$ ).<sup>6</sup> One of the key issues addressed in these studies was the assignment of the

arene hapticity in the odd-electron intermediate in such processes. NMR data showed that the  $\text{Rh}(\text{II})$  intermediate  $[\text{Cp}^*\text{Rh}(\eta\text{-C}_6\text{Me}_6)]^+$  has a planar  $\eta^6\text{-arene}$  structure and is, therefore, a 19e complex.<sup>7</sup> A recent review article on this problem suggests that the existence of such hypervalent intermediates is more widespread than is commonly assumed.<sup>8</sup>

Given their facile  $\eta^5 \rightarrow \eta^3$  ring-slippage rearrangements, indenyl complexes may be considered as good candidates to undergo reversible 2e redox transformations. The first documented example of this behavior was reported by Trogler and concerns the electrochemically reversible stepwise reduction of  $[(\eta^5\text{-Ind})_2\text{V}(\text{CO})_2]^+$  to  $[(\eta\text{-Ind})_2\text{V}(\text{CO})_2]^-$ ,<sup>9a</sup> for which the intermediate was structurally characterized by X-ray studies as the ring-slipped 17e species  $(\eta^5\text{-Ind})(\eta^3\text{-Ind})\text{V}(\text{CO})_2$ .<sup>9b</sup> The analogues  $[\text{Cp}'_2\text{V}(\text{CO})_2]^+$  ( $\text{Cp}' = \text{Cp}$ ,  $\text{Cp}^*$ ) show a totally irreversible decomposition under the same conditions. More recently, Cooper reported the chemical, spectroscopical, and electrochemical study of the system  $[\text{IndMn}(\text{CO})_3]^{0/-2-}$ . The expected  $\eta^3\text{-Ind}$  coordination is assigned to the dianion (18e species), but the electrochemical evidence supports the 19e monoanionic intermediate  $[\text{IndMn}(\text{CO})_3]^-$  with  $\eta^5\text{-Ind}$  coordination.<sup>10</sup> In close parallel, the 2e reduction of  $[\text{IndFe}(\text{CO})_3]^+$  occurs in a stepwise fashion to give ultimately the anion  $[(\eta^3\text{-$

<sup>†</sup> Instituto de Tecnologia Química e Biológica da Universidade Nova de Lisboa.

<sup>‡</sup> Instituto Politécnico de Setúbal.

<sup>§</sup> Technische Universität München.

(1) Fischer, E. O.; Elschenbroich, C. *Chem. Ber.* **1970**, *103*, 162.

(2) Hüttner, G.; Lange, S. *Acta Crystallogr., Sect. B* **1972**, *B28*, 2049.

(3) (a) Finke, R. G.; Voegeli, R. H.; Langanis, E. D.; Boekelheide, V. *Organometallics* **1983**, *2*, 347. (b) Langanis, E. D.; Voegeli, R. H.; Swann, R. T.; Finke, R. G.; Hopf, H.; Boekelheide, V. *Organometallics* **1982**, *1*, 1415. (c) Plitzko, K. D.; Wehrle, G.; Gollas, B.; Rapko, B.; Dannheim, J.; Boekelheide, V. *J. Am. Chem. Soc.* **1990**, *112*, 6556.

(4) Pierce, D. T.; Geiger, W. E. *J. Am. Chem. Soc.* **1992**, *114*, 6063.

(5) Nielson, R. M.; Weaver, M. J. *Organometallics* **1989**, *8*, 1636.

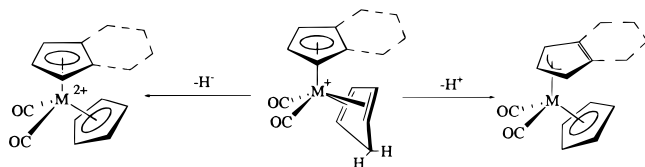
(6) (a) Bowyer, W. J.; Geiger, W. E. *J. Am. Chem. Soc.* **1985**, *107*, 5657. (b) Bowyer, W. J.; Geiger, W. E. *J. Electroanal. Chem. Interfacial Electrochem.* **1988**, *239*, 253. (c) Bowyer, W. J.; Merkert, J. W.; Geiger, W. E.; Rheingold, A. L. *Organometallics* **1989**, *8*, 191.

(7) Merkert, J.; Nielson, R. M.; Weaver, M. J.; Geiger, W. E. *J. Am. Chem. Soc.* **1989**, *111*, 7084.

(8) Geiger, W. E. *Acc. Chem. Res.* **1995**, *28*, 351.

(9) (a) Miller, G. A.; Therien, M. J.; Trogler, W. C. *J. Organomet. Chem.* **1990**, *383*, 271. (b) Kowaleski, R. M.; Rheingold, A. L.; Trogler, W. C.; Basolo, F. *J. Am. Chem. Soc.* **1986**, *108*, 2460.

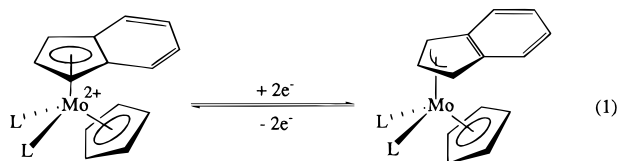
(10) Lee, S.; Lovelace, S. R.; Cooper, N. J. *Organometallics* **1995**, *14*, 1974.

**Scheme 1.**  $\text{H}^-$  Abstraction and  $\text{H}^+$  Abstraction from  $[\text{Cp}^*\text{M}(\eta^4\text{-C}_5\text{H}_6)(\text{CO})_2]^+$ 

$\text{Ind})\text{Fe}(\text{CO})_3]^-$ .<sup>11</sup> Again, the neutral intermediate is assigned as a 19e species and, therefore, to have  $\eta^5$ -indenyl coordination. On the other hand, the electrochemical evidence obtained on the reduction of  $(\eta^5\text{-Ind})\text{Rh}(\text{COD})$  does not allow for a clear distinction between a 17e and 19e configurations for the anion  $[(\eta\text{-Ind})\text{Rh}(\text{COD})]^-$ .<sup>12</sup>

We have recently characterized the dications  $[\text{Cp}_2\text{M}(\text{CO})_2]^{2+}$  and  $[\text{IndCpM}(\text{CO})_2]^{2+}$  ( $\text{M} = \text{Mo}, \text{W}$ ) and independently synthesized their ring-slipped reduced analogues  $(\eta^3\text{-Cp})(\eta^5\text{-Cp})\text{M}(\text{CO})_2$  and  $(\eta^3\text{-Ind})\text{CpM}(\text{CO})_2$ , as shown in Scheme 1.<sup>13</sup>

Preliminary experiments revealed that the cyclic voltammogram of  $[\text{IndCpW}(\text{CO})_2]^{2+}$  presents only a reversible 2e reduction wave in NCMe, whereas chemical oxidation of  $(\eta^3\text{-Ind})\text{CpM}(\text{CO})_2$  forms the dications  $[\text{IndCpM}(\text{CO})_2]^{2+}$ . These results suggest the possibility of generating a variety of closely related complexes which might undergo two successive one-electron redox steps according to eq 1. This was found to be possible and we now present the synthesis of a variety of dications  $[\text{IndCpML}_2]^{2+}$  and their direct reductions to the indenyl-slipped neutral complexes  $(\eta^3\text{-Ind})\text{CpML}_2$ .



## Results

**Chemical Studies.** The synthesis of the dications is summarized in Scheme 2 and uses the previously reported precursors  $[\text{IndCpMo}(\text{CO})_2]^{2+}$ ,  $\text{IndCpMoCl}_2$ , and  $[\text{IndCpMo}(\text{NCMe})_2]^{2+}$ .<sup>13</sup>

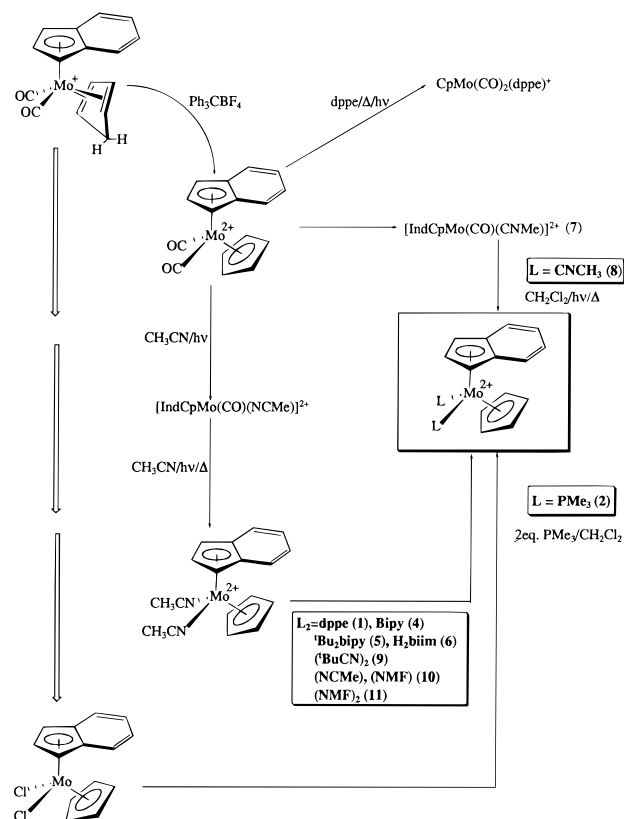
Generally speaking, the dications are easily isolated as analytically pure crystalline materials. The  $^1\text{H}$  NMR chemical shifts of the indenyl protons in the  $\eta^5$ -coordination mode assumed for 18e compounds **1–11** (Table 1) follow the reported pattern for similar complexes: two multiplets for  $\text{H}^{5-8}$  ( $\delta$  8–6.5 ppm), a doublet for  $\text{H}^{1/3}$  ( $\delta$  7–5.5 ppm) and a triplet for  $\text{H}^2$  ( $\delta$  6.5–5.5 ppm).<sup>14</sup>

(11) Pevear, K. A.; Banaszak Holl, M. M.; Carpenter, G. B.; Rieger, A. L.; Rieger, P. H.; Sweigart, D. A. *Organometallics* **1995**, *14*, 512 and references therein.

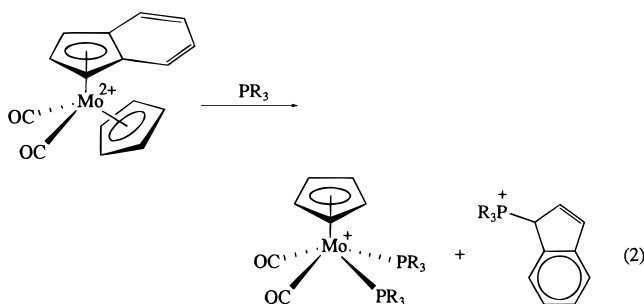
(12) Amatore, C.; Ceccon, A.; Santi, S.; Verpeaux, J.-N. *Chem. Eur. J.* **1997**, *3*, 279.

(13) (a) Ascenso, J. R.; de Azevedo, C. G.; Gonçalves, I. S.; Herdtweck, E.; Moreno, D. S.; Romão, C. C.; Zühlke, J. *Organometallics* **1994**, *13*, 429. (b) Ascenso, J. R.; de Azevedo, C. G.; Gonçalves, I. S.; Herdtweck, E.; Moreno, D. S.; Pessanha, M.; Romão, C. C. *Organometallics* **1995**, *14*, 3901. (c) Gonçalves, I. S.; Romão, C. C. *J. Organomet. Chem.* **1995**, *48*, 155.

(14) Calhorda, M. J.; Gamelas, C. A.; Gonçalves, I. S.; Herdtweck, E.; Romão, C. C.; Veiros, L. F. *Organometallics* **1998**, *17*, 2597.

**Scheme 2**

The choice of the most adequate starting material depends on its own reactivity toward the nucleophiles  $\text{L}$ . The rings of the more accessible dication  $[\text{IndCpMo}(\text{CO})_2][\text{BF}_4]_2$  are very reactive toward strong nucleophiles such as phosphines. Therefore, its synthetic use in this context was limited to the preparation of the nitrile precursor  $[\text{IndCpMo}(\text{NCMe})_2]^{2+}$  and isonitrile complexes **7** and **8**, all of which are the result of slow CO substitutions. Reaction of  $[\text{IndCpMo}(\text{CO})_2][\text{BF}_4]_2$  with  $\text{dppe}$  under reflux and visible-light irradiation gives the analytically pure complex  $[\text{CpMo}(\text{CO})_2(\text{dppe})][\text{BF}_4]$ ,<sup>16</sup> with a Cp signal at  $\delta$  4.75 ppm. The weaker nucleophile  $\text{P}(\text{OMe})_3$  affords similar results.<sup>15</sup> Both reactions correspond to a loss of the indenyl ring, which can be interpreted as the result of nucleophilic addition of the phosphines to the indenyl ring followed by replacement of the resulting  $[\text{R}_3\text{P}(\text{Ind})]^+$  ligand by excess phosphine, as in eq 2.



A similar attack at the indenyl ring takes place during the reaction of  $\text{IndCpMoCl}_2$  with excess  $\text{PMe}_3$  and  $\text{TIBF}_4$

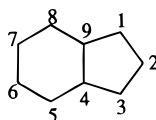
(15) Félix, V.; Drew, M., personal communication, 1997.

(16) Green, M. L. H.; Knight, J.; Segal, J. A. *J. Chem. Soc., Dalton Trans.* **1977**, 2189.

**Table 1.** Selected  $^1\text{H}$  and  $^{13}\text{C}$  NMR Data for  $[(\eta^5\text{-Ind})\text{CpMoL}_2][\text{BF}_4]_2$  and Related Compounds<sup>a</sup>

complex	ligand	chem shift of $\eta^5\text{-Ind}$ ligand ( $\delta$ (ppm); room temp)				ref
		$\text{H}^{5-8}$	$\text{H}^{1/3}$	$\text{H}^2$	$\text{C}^{4/9}$	
<b>1</b>	dppe <sup>b</sup>	7.39; 6.64 m	5.55 m	6.27 m	112.4	this work
<b>2</b>	(PMe <sub>3</sub> ) <sub>2</sub> <sup>b</sup>	7.67 s	5.99 m	5.45 m	112.3	this work
<b>4</b>	Bipy	7.69; 7.34 m	6.34 d	6.63 t	116.2	this work
<b>5</b>	<sup>t</sup> Bu <sub>2</sub> bipy	7.52; 7.18 m	6.14 d	6.43 t		this work
<b>6</b>	H <sub>2</sub> biim	7.57; 7.43 m	6.20 d	6.57 t	123.5	this work
<b>7</b>	(CO)(CNMe) <sup>b</sup>	7.82 m	6.70 c	6.32 t		this work
<b>8</b>	(CNMe) <sub>2</sub> <sup>b</sup>	7.70 m	6.34 d	6.05 t	112.8	this work
<b>9</b>	(CN <sup>t</sup> Bu) <sub>2</sub>	7.99; 7.83 m	6.81 d	6.37 t	112.7	this work
<b>10</b>	(NCMe)(NMF)	7.90; 7.73 m	6.71 d	6.65 t		this work
<b>11</b>	(NMF) <sub>2</sub>	7.66; 7.60 s	6.46 d	6.53 t		this work
M = Mo	(CO) <sub>2</sub>	8.27; 8.09 m	7.55 d	6.98 t		12
	(P(OMe) <sub>3</sub> ) <sub>2</sub>	7.92; 7.80 m	6.34 m	6.29 m	112.4	14
	(CO)(NCMe)	7.85; 7.78 m	6.93; 6.22 m	6.39 t		12
M = W	(NCMe) <sub>2</sub>	7.59 s	5.92 d	6.65 t		12

<sup>a</sup> All spectra in CD<sub>3</sub>COCD<sub>3</sub> except as noted. Legend: dppe = 1,2-bis(diphenylphosphino)ethane, Bipy = 2,2'-bipyridyl, <sup>t</sup>Bu<sub>2</sub>bipy = 4,4'-di-*tert*-butyl-2,2'-bipyridine, H<sub>2</sub>biim = bis(imidazole), CN<sup>t</sup>Bu = *tert*-butyl isocyanide, NMF = *N*-methylformamide. The numbering scheme is as follows:



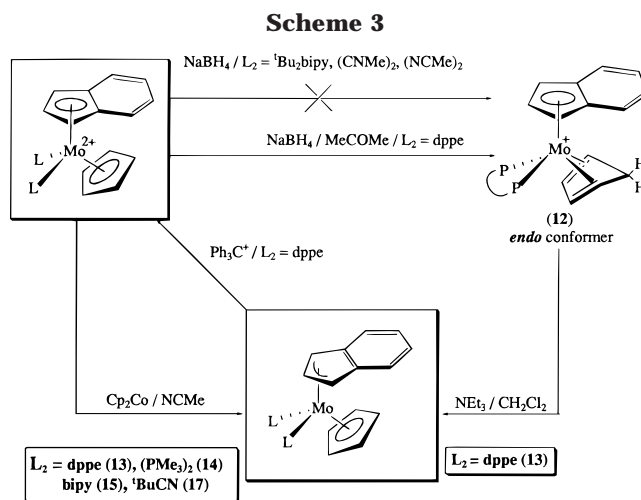
<sup>b</sup> Spectrum in CD<sub>3</sub>CN.

in acetone, affording the cation  $[\text{CpMo}(\text{PMe}_3)_4]\text{BF}_4$  (**3**). This reaction is certainly mediated by some cationic species with a high reactivity toward ring addition. In the less ionizing solvent CH<sub>2</sub>Cl<sub>2</sub>, phosphine attack at the indenyl ring was prevented and the desired dication  $[\text{IndCpMo}(\text{PMe}_3)_2][\text{BF}_4]_2$  (**2**) was isolated in 70% yield. However, these problems are best avoided by the use of the labile nitrile dication  $[\text{IndCpMo}(\text{NCMe})_2][\text{BF}_4]_2$ , which proved to be the most convenient synthetic precursor. Its insolubility in CH<sub>2</sub>Cl<sub>2</sub> was overcome by adding a small amount of NMF (*N*-methylformamide) to the reaction mixture, thereby catalyzing the substitution reactions when L is 1,2-bis(diphenylphosphino)ethane (dppe), PMe<sub>3</sub>, 2,2'-bipyridine (Bipy), <sup>t</sup>Bu<sub>2</sub>bipy, 2,2'-bis(imidazole) (H<sub>2</sub>biim), CNMe, and CN<sup>t</sup>Bu. In fact, in the absence of NMF some of the preparations reported in this work do not occur (e.g. preparation of **8**). Nitrile substitution by NMF occurs readily, and the NMF complexes **10** and **11** were isolated and characterized. The lability of NMF in complex **10** was demonstrated by the  $^1\text{H}$  NMR observation of its facile conversion into  $[\text{IndCpMo}(\text{NCCD}_3)_2][\text{BF}_4]_2$  at room temperature, immediately after dissolution in NCCD<sub>3</sub>.

<sup>31</sup>P coupling to the indenyl protons is evident in the  $^1\text{H}$  NMR spectra of **1** and **2**, H<sup>1/3</sup> and H<sup>2</sup> appearing as multiplets (instead of a doublet and a triplet). Concomitantly, the signal of the Cp ring in these complexes appears as a triplet, as in  $[\text{Cp}_2\text{Mo}(\text{dppe})]^{2+}$ .<sup>17,18</sup>

The crystal structure of  $[\text{IndCpMo}(\text{dppe})][\text{BF}_4]_2$  (**1**) confirms the expected planar  $\eta^5$ -coordination mode of the indenyl ligand (see Crystallography).

In contrast to the above-mentioned addition of the phosphines to the indenyl ring of  $[\text{IndCpMo}(\text{CO})_2]^{2+}$ , H<sup>-</sup> adds to the Cp ring of the dication **1**, affording the diene complex  $[\text{IndMo}(\eta^4\text{-C}_5\text{H}_6)(\text{dppe})]\text{BF}_4$  (**12**). Also, in con-



trast to its carbonyl analogue  $[\text{IndMo}(\eta^4\text{-C}_5\text{H}_6)(\text{CO})_2]\text{BF}_4$ , **12** is not fluxional, as can be concluded by the invariance of its  $^1\text{H}$  NMR spectrum with temperature (from -80 °C to room temperature). **12** was assigned as the *endo* conformer (bridgehead CH<sub>2</sub> *cis* to the indenyl ring as in Scheme 3) by comparison of its  $^1\text{H}$  NMR spectrum with the one of the known congener  $[\text{CpMo}(\eta^4\text{-C}_5\text{H}_6)(\text{dppe})]\text{BF}_4$ .<sup>18</sup> In fact, the chemical shifts of the methylene protons of the C<sub>5</sub>H<sub>6</sub> ring are very similar to those observed for  $[\text{CpMo}(\eta^4\text{-C}_5\text{H}_6)(\text{dppe})]\text{BF}_4$  and, therefore, we assigned H<sub>endo</sub> as the higher field resonance at  $\delta$  2.85 ppm and H<sub>exo</sub> as the lower field resonance at  $\delta$  3.32 ppm (see Experimental Section). As expected, H<sub>exo</sub> in **12** exhibits a distinct IR stretching vibration at 2768 cm<sup>-1</sup>.

Hydride addition to **4**, **5**, **8**, and  $[\text{IndCpMo}(\text{NCMe})_2][\text{BF}_4]_2$  proved to be unsuccessful for the preparation of the respective diene complexes, probably due to attack at the non-hydrocarbon unsaturated ligands.

$[\text{IndMo}(\eta^4\text{-C}_5\text{H}_6)(\text{dppe})]\text{BF}_4$  (**12**) was readily deprotonated by NEt<sub>3</sub>, yielding the neutral species ( $\eta^3\text{-Ind}$ )-CpMo(ddpe) (**13**), as depicted in Scheme 3.

(17) Aviles, T.; Green, M. L. H.; Dias, A. R.; Romão, C. C. *J. Chem. Soc., Dalton Trans.* **1979**, 1367.

(18) de Azevedo, C. G.; Calhorda, M. J.; de C. T. Carrondo, M. A. A. F.; Dias, A. R.; Duarte, M. T.; Galvão, A. M.; Gamelas, C. A.; Gonçalves, I. S.; da Piedade, F. M.; Romão, C. C. *J. Organomet. Chem.* **1997**, 544, 257.



**Table 2. Selected  $^1\text{H}$  and  $^{13}\text{C}$  NMR Data for  $(\eta^3\text{-Ind})\text{CpMoL}_2$  and Related Compounds<sup>a</sup>**

complex	ligand	chem shift of $\eta^3\text{-Ind}$ ligand ( $\delta$ (ppm); room temp)				ref
		$\text{H}^{5-8}$	$\text{H}^{1/3}$	$\text{H}^2$	$\text{C}^{4/9}$	
<b>13</b>	dppe	6.46 d	2.96 s (br)	5.96 s (br)	151.5	this work
<b>14</b>	( $\text{PMe}_3$ ) <sub>2</sub>	6.52 s (br)	3.03 s (br)	6.26 s (br)		this work
<b>15</b>	Bipy	6.78; 6.68 m	4.77 d	3.44 s (br)		this work
<b>16</b>	(CO)(CNMe)	7.16; 6.88 6.65; 6.51	4.85; 4.62 t	5.50 m		this work
<b>17</b>	( $\text{CN}^t\text{Bu}$ ) <sub>2</sub>	6.63; 6.50 m	4.41 d	6.81 t		this work
M = Mo	(CO) <sub>2</sub>	6.56 m	5.21 d	6.75 t	151.1	12
	( $\text{P}(\text{OMe})_3$ ) <sub>2</sub>	6.54 m	3.89 m	3.89 m	157.5	14
	( $\eta^3\text{-Ind}$ )(CO) <sub>2</sub>	6.68 m	5.11 d	4.80 t		12
M = W	(CO) <sub>2</sub>	6.56 m	4.95 d	7.07 t	152.0	18

<sup>a</sup> All spectra at room temperature in  $\text{C}_6\text{D}_6$ . See Table 1 for numbering.

**Table 3. Cyclic Voltammetry Data**

complex <sup>a</sup>	ligand	$E_{\text{p,a}}$ (V)	$E_{\text{p,c}}$ (V)	$E_{\text{p}/2}$ (V)	$I_{\text{a}}/I_{\text{c}}$
$\eta^5\text{-Ind}$					
<b>1</b>	dppe	-0.30; -0.46	-0.37; -0.52	-0.34; -0.49	1.0; 0.9
<b>2</b>	( $\text{PMe}_3$ ) <sub>2</sub>	-0.46; -0.74	-0.53; -0.81	-0.50; -0.78	1.0; 1.0
<b>4</b>	Bipy	-0.59	-0.67	-0.63	0.9
<b>5</b>	$t\text{Bu}_2\text{bipy}$	-0.60	-0.68	-0.64	1.0
<b>6</b>	$\text{H}_2\text{biim}$	-0.90; -1.16	-0.99; -1.26	-0.94; -1.21	1.0; 1.1
<b>7</b>	(CO)(CNMe)	-0.15	-0.22	-0.19	1.1
<b>8</b>	(CNMe) <sub>2</sub>	-0.53	-0.61	-0.57	0.9
<b>9</b>	(CNCMe) <sub>2</sub>	-0.49	-0.57	-0.53	1.0
<b>12<sup>b</sup></b>	( $\eta^4\text{-C}_5\text{H}_6$ )(dppe)	+1.27; +0.77			
$\eta^3\text{-Ind}$					
<b>13</b>	dppe	-0.29; -0.46	-0.36; -0.52	-0.33; -0.49	1.0; 0.9
<b>14</b>	( $\text{PMe}_3$ ) <sub>2</sub>	-0.46; -0.74	-0.53; -0.81	-0.50; -0.78	1.0; 1.0
<b>15</b>	Bipy	-0.59	-0.66	-0.63	1.0
<b>17</b>	(CNCMe) <sub>2</sub>	-0.49	-0.56	-0.53	1.0
M = Mo	(CO) <sub>2</sub>	0.19	$E_{\text{p,c}}(1) = 0.12$ $E_{\text{p,c}}(2) = -0.26$ $E_{\text{p,c}}(3) = -0.90$	irrev	

<sup>a</sup> All the voltammograms were measured in NCMe, except as noted, in ca. 1.0 mM solutions at a scan rate of 200 mV/s and room temperature.  $E_{\text{p,a}}$ ,  $E_{\text{p,c}}$ , and  $E_{\text{p}/2}$  are referenced to SCE on the basis of a simultaneous measurement of the ferrocene redox potential (+0.444 V for  $\text{CH}_2\text{Cl}_2$  and +0.400 V for NCMe).  $E_{\text{p,a}}$  = anodic sweep (peak potentials).  $E_{\text{p,c}}$  = cathodic sweep (peak potentials).  $E_{\text{p}/2}$  = half-wave potential ( $(E_{\text{p,a}} + E_{\text{p,c}})/2$ ).  $I_{\text{a}}$  = anodic current intensity.  $I_{\text{c}}$  = cathodic current intensity. <sup>b</sup> Measured in  $\text{CH}_2\text{Cl}_2$ .

$^1\text{H}$  NMR in  $\text{C}_6\text{D}_6$  confirms the  $\eta^3$ -indenyl coordination with the  $\text{H}^{1/3}$  resonance (a broad singlet at  $\delta$  2.96 ppm) and the  $\text{H}^{5-8}$  resonance (a doublet at  $\delta$  6.46 ppm) shifted upfield relative to their usual positions in the  $\eta^5$ -indenyl coordination mode.<sup>14</sup> The  $\text{C}_5$  ring appears at  $\delta$  4.48 ppm.

The structure of complex **13** was confirmed by X-ray diffraction analysis of a single crystal (see Crystallography).

( $\eta^3\text{-Ind}$ )CpMo(dppe) (**13**) proved to be resistant to electrophilic addition of HCl in  $\text{Et}_2\text{O}$  and of MeI in toluene, at room temperature. Reaction of this neutral complex with  $\text{Ph}_3\text{CBF}_4$  in  $\text{CH}_2\text{Cl}_2$  results in oxidation, affording the dication **1**. Conversely, reduction of **1** with  $\text{Cp}_2\text{Co}$  produces **13** in 95% yield.

The dications **2**, **4**, **7**, and **9** also undergo similar reductions with  $\text{Cp}_2\text{Co}$  to give the ring-slipped neutral species **14**–**17**, as depicted in Scheme 3. However, this general synthetic procedure does not produce either ( $\eta^3\text{-Ind}$ )CpMo(NCMe)<sub>2</sub> or ( $\eta^3\text{-Ind}$ )CpMo(CNMe)<sub>2</sub>. Unidentified decomposition products are formed instead.

The  $^1\text{H}$  NMR chemical shifts of the protons of the slipfolded  $\eta^3$ -indenyl rings of compounds **13**–**17** follow two distinct patterns (Table 2). The most general one has also been reported for the bis(indenyl) complex ( $\eta^5\text{-Ind}$ )-( $\eta^3\text{-Ind}$ )Mo(CO)<sub>2</sub><sup>13</sup> and shows the  $\text{H}^2$  and  $\text{H}^{1/3}$  resonances shifted upfield from their typical positions in the related  $\eta^5$  coordination mode. This is the case for the complexes with dppe (**13**),  $\text{PMe}_3$  (**14**), Bipy (**15**), and (CO)(CNMe)

(**16**). A second pattern is found for the  $\text{CN}^t\text{Bu}$  derivative (**17**). In this case, the  $^1\text{H}$  NMR spectrum is similar to that of ( $\eta^3\text{-Ind}$ )CpMo(CO)<sub>2</sub>: a triplet for  $\text{H}^2$  (ca.  $\delta$  6.8 ppm), two multiplets for  $\text{H}^{5-8}$  (ca.  $\delta$  6.5 ppm), and a doublet for  $\text{H}^{1/3}$  (ca.  $\delta$  4.5 ppm).<sup>13</sup> The asymmetric complex ( $\eta^3\text{-Ind}$ )CpMo(CO)(CNMe) (**16**) exhibits four signals for  $\text{H}^{5-8}$  as previously observed in other asymmetric indenyl molybdenocene derivatives, such as [IndCpMo(CO)Cl][ $\text{BF}_4$ ].<sup>13</sup>

All  $^1\text{H}$  NMR peaks in  $\text{C}_6\text{D}_6$  are sharp at room temperature. The rather broad signals observed at room temperature in the  $\text{CD}_2\text{Cl}_2$  spectrum of dppe complex **13** become well-resolved at  $-70^\circ\text{C}$ . We did not attempt any study of this behavior, due to the slow reaction of the complex with  $\text{CD}_2\text{Cl}_2$ .

**Electrochemical Studies.** The cyclic voltammograms of the dications  $[\text{IndCpMoL}_2]^{2+}$  (**1**–**9**) and their reduced ring-slipped counterparts  $[(\eta^3\text{-Ind})\text{CpMoL}_2]$  (**13**–**17**) as well as a few other related complexes were studied in NCMe and  $\text{CH}_2\text{Cl}_2$ , and the data are summarized in Table 3 and Figure 1.

The cyclic voltammograms of dications **4**, **5**, and **7**–**9** show one 2e quasi-reversible wave, as in  $[\text{IndCpW}(\text{CO})_2]^{2+}$ ,<sup>13</sup> that can be attributed to the two consecutive

(19) Gonçalves, I. S.; Romão, C. C. *J. Organomet. Chem.* **1995**, *48*, 155.

(20) Amatore, C.; Azzabi, M.; Calas, P.; Jutand, A.; Lefrou, C.; Rollin, Y. *J. Electroanal. Chem. Interfacial Electrochem.* **1990**, *288*, 45.

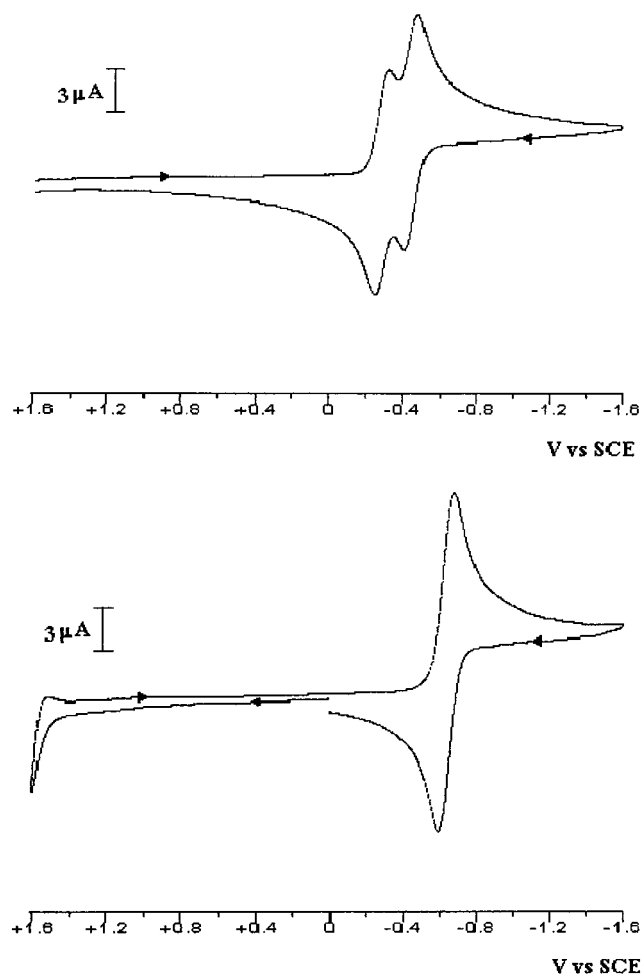


**Figure 1.** (a, top) Cyclic voltammogram of [IndCpMo(dppe)][BF<sub>4</sub>]<sub>2</sub> (**1**) in NCMe. A similar wave pattern is observed for **2** and **6** (see Table 3 for CV data). (b, bottom) Cyclic voltammogram of [IndCpMo(Bu<sub>2</sub>bipy)][BF<sub>4</sub>]<sub>2</sub> (**5**) in NCMe. A similar wave pattern is observed for **4**, **7**, **8**, and **9** (see Table 3 for CV data).

electron transfer reactions from Mo(IV) to Mo(II). The electron count was performed according to a published method.<sup>20</sup> Cyclic voltammograms of dications **1**, **2**, and **6** show that these complexes undergo two distinct quasi-reversible 1e reduction steps. The ring-slipped complexes ( $\eta^3$ -Ind)CpMo(dppe) (**13**), ( $\eta^3$ -Ind)CpMo(PMe<sub>3</sub>)<sub>2</sub> (**14**), and ( $\eta^3$ -Ind)CpMo(bipy) (**15**) present cyclic voltammograms similar to those for the respective dications, **1**, **2**, and **4**. The previously reported congener of complex **1** [Cp<sub>2</sub>Modppe]<sup>2+</sup> presents only irreversible oxidation waves (at 0.43, 0.78, and 1.28 V).<sup>18</sup>

In keeping with the chemical observations of the reductions with Cp<sub>2</sub>Co, the [IndCpMo(NCMe)<sub>2</sub>]<sup>2+</sup> complex presents irreversible reduction waves. In contrast, [IndCpMo(CNMe)<sub>2</sub>]<sup>2+</sup>, which cannot be chemically reduced with Cp<sub>2</sub>Co to ( $\eta^3$ -Ind)CpMo(CNMe)<sub>2</sub>, shows an electrochemical reversibility similar to that of the other dications, for example [IndCpMo(CN<sup>t</sup>Bu)<sub>2</sub>]<sup>2+</sup> (**9**).

The relative shift of the peak potentials reflects the variations in the overall donor/acceptor abilities of the L<sub>2</sub> ligands. This is clearly illustrated by comparison of the potentials of the two phosphine derivatives **1** and **2**, the latter (L = PMe<sub>3</sub>) being, as expected, more difficult to reduce than the former (L<sub>2</sub> = dppe), which bears a weaker  $\sigma$  donor and a better  $\pi$  acceptor.

**Table 4. Crystallographic Data for [( $\eta^5$ -Ind)CpMo(dppe)]<sup>2+</sup>[BF<sub>4</sub>]<sup>-</sup><sub>2</sub>·3CH<sub>3</sub>CN (**1**) and [( $\eta^3$ -Ind)CpMo(dppe)] (**13**)**

	<b>1</b>	<b>13</b>
chem formula	C <sub>46</sub> H <sub>45</sub> B <sub>2</sub> F <sub>8</sub> MoN <sub>3</sub> P <sub>2</sub>	C <sub>40</sub> H <sub>36</sub> MoP <sub>2</sub>
fw	971.38	674.61
color/shape	dark red/column	orange/prism
cryst size (mm)	0.69 × 0.25 × 0.25	0.28 × 0.20 × 0.13
cryst syst	monoclinic	triclinic
space group	P2 <sub>1</sub> /c	P1
a (pm)	1409.84(5)	1092.50(2)
b (pm)	1381.67(8)	1267.18(4)
c (pm)	2237.82(9)	1322.68(4)
$\alpha$ (deg)	90	112.770(1)
$\beta$ (deg)	95.992(4)	94.081(2)
$\gamma$ (deg)	90	108.926(2)
V (10 <sup>6</sup> pm <sup>3</sup> )	4335.3(3)	1555.98(8)
Z	4	2
T (K)	193	173
$\rho_{\text{calcd}}$ (g cm <sup>-3</sup> )	1.488	1.440
$\mu$ (cm <sup>-1</sup> )	4.5	5.5
F <sub>000</sub>	1984	696
$\lambda$ (pm)	71.073	71.073
scan method	imaging plate	kappa CCD
$\theta$ range (deg)	2.32–27.75	2.18–31.35
data collcd (hkl)	±16, ±18, ±29	±12, ±18, ±18
no. of rflns collcd	36 076	14 111
no. of indep rflns	9536	7231
no. of obsd rflns	9536 (all data)	7231(all data)
no. of params refined	571	532
R <sub>int</sub>	0.025	0.026
R1 <sup>a</sup>	0.0424	0.0306
wR2 <sup>b</sup>	0.0905	0.0709
GOF <sup>c</sup>	1.035	1.071
$\Delta\rho_{\text{max/min}}$ (e Å <sup>-3</sup> )	+0.75, -0.50	+0.39, -0.39

<sup>a</sup> R1 =  $\sum(|F_o| - |F_c|)/\sum|F_o|$ . <sup>b</sup> wR2 =  $[\sum w(F_o^2 - F_c^2)^2/\sum w(F_o^2)^2]^{1/2}$ . <sup>c</sup> GOF =  $[\sum w(F_o^2 - F_c^2)^2/(\text{NO} - \text{NV})]^{1/2}$ ; w = SHELXL-93 weights.

A smaller difference is observed between the two isonitrile complexes **8** and **9**, the latter (L = CN<sup>t</sup>Bu) being, as expected, slightly more difficult to reduce than the former. Particularly striking is the negative potential of the bis(imidazole) complex **6**, clearly more negative than the potentials of the bipyridyl derivatives **4** and **5**.

The CO complexes are the easiest to reduce in the whole series (although irreversibly). This is certainly due to the high capacity of the CO ligand to withdraw charge from the reduced metal center by back-donation.

**Crystallography.** **1** and **13** were further characterized by single-crystal X-ray diffraction crystallography, and the corresponding data are given in Table 4. Key bond distances and angles together with the characteristic slip parameters of the indenyl ligand are listed in Table 5.

Both compounds (Figures 2 and 3) are monomeric, and the geometry around the metal atom is best described by a distorted tetrahedron. Complex **1** has the typical structure of a molybdenocene derivative, and **13** has a structure similar to that of many allylic complexes of the type CpMo( $\eta^3$ -allyl)(CO)<sub>2</sub>. A projection on the Mo, P(1), and P(2) plane (Figures 2a and 3a) shows that the Cp ring adopts an approximately staggered conformation in **1** and an eclipsed conformation in **13**. The average Mo–P distance in **1** (250.7(1) pm) is significantly longer than in complex **13** (242.6(1) pm), which in turn is very similar to that for the isoelectronic allylic complex CpMo( $\eta^3$ -C<sub>5</sub>H<sub>7</sub>)(dppe) (242.1(2) pm)<sup>18</sup> and to that for the Mo(II) complex ( $\eta^5$ -C<sub>5</sub>Me<sub>5</sub>)Mo(dppe)Cl (242.8(1) pm).<sup>21</sup> All intramolecular distances and angles fall

**Table 5. Selected Interatomic Distances (pm), Angles (deg), and Slip Parameters<sup>a</sup> for  $[(\eta^5\text{-Ind})\text{CpMo}(\text{dppe})]^{2+}[\text{BF}_4]^{-2} \cdot 3\text{CH}_3\text{CN}$  (**1**) and  $[(\eta^3\text{-Ind})\text{CpMo}(\text{dppe})]$  (**13**)**

	<b>1</b> <sup>b</sup>	<b>13</b> <sup>c</sup>
Mo–C( <i>m</i> 1)	235.7(3)	236.5(2)
Mo–C( <i>m</i> 2)	230.3(3)	233.7(2)
Mo–C( <i>m</i> 3)	228.6(3)	229.7(2)
Mo–C( <i>m</i> 4)	232.1(2)	230.4(2)
Mo–C( <i>m</i> 5)	237.8(3)	232.2(2)
Mo–C( <i>n</i> 1)	229.3(3)	231.0(2)
Mo–C( <i>n</i> 2)	222.6(2)	218.4(2)
Mo–C( <i>n</i> 3)	229.3(2)	235.1(2)
Mo–C( <i>n</i> 3A)	242.7(2)	302.6(2)
Mo–C( <i>n</i> 7A)	242.9(2)	305.5(2)
Mo–P(1)	250.83(5)	242.00(6)
Mo–P(2)	250.52(5)	243.12(5)
C( <i>n</i> 1)–C( <i>n</i> 2)	142.8(3)	142.9(3)
C( <i>n</i> 1)–C( <i>n</i> 7A)	142.0(3)	147.5(3)
C( <i>n</i> 2)–C( <i>n</i> 3)	143.0(3)	144.3(4)
C( <i>n</i> 3)–C( <i>n</i> 3A)	141.6(3)	146.2(3)
C( <i>n</i> 3A)–C( <i>n</i> 4)	142.8(3)	138.5(4)
C( <i>n</i> 3A)–C( <i>n</i> 7A)	143.4(3)	142.6(3)
C( <i>n</i> 4)–C( <i>n</i> 5)	135.3(3)	140.4(3)
C( <i>n</i> 5)–C( <i>n</i> 6)	142.8(4)	138.5(4)
C( <i>n</i> 6)–C( <i>n</i> 7)	135.2(4)	140.7(4)
C( <i>n</i> 7)–C( <i>n</i> 7A)	142.9(3)	137.8(3)
P(1)–Mo–P(2)	78.53(2)	78.26(2)
P(1)–Mo–C(ind)	109.0	97.3
P(1)–Mo–Cp	105.5	115.9
P(2)–Mo–C(ind)	110.3	94.7
P(2)–Mo–Cp	103.8	125.4
C(ind)–Mo–Cp	135.2	130.9

	<b>1</b>		<b>13</b>	
	indenyl	Cp	indenyl	Cp
$\Delta =  \sigma $ (pm)	22.2	9.3	110.2	7.0
$\sigma$ (deg)	0.7	14.2	7.4	29.4
$\Psi$ (deg)	6.4	2.7	28.5	2.0
$\Delta M-C$ (pm)	15.7	6.3	75.9	4.3
$\Omega$ (deg)	2.5	1.7	25.0	1.6

<sup>a</sup> Slip parameters are defined in refs 22 and 37. <sup>b</sup> *m* = 5, *n* = 6; C(ind) denotes the centroid C(61–67A); Cp denotes the centroid C(51–55). <sup>c</sup> *m* = 2, *n* = 1; C(ind) denotes the centroid C(11–13); Cp denotes the centroid C(21–25).

within the ranges observed for related compounds, for example (a) the Mo–P distances, 246.4(2) pm in  $(\text{d}^2)\text{-}[(\eta^5\text{-Ind})(\text{Cp})\text{Mo}\{\text{P}(\text{OMe})_3\}_2]^{2+}$  and 239.1(2) pm in  $(\text{d}^4)\text{-}[(\eta^3\text{-Ind})(\text{Cp})\text{Mo}\{\text{P}(\text{OMe})_3\}_2]^{2+}$ ,<sup>15</sup> (b) the P(1)–Mo–P(2) angle of 78.71(4)° in  $(\eta^5\text{-C}_5\text{Me}_5)\text{Mo}(\text{dppe})\text{Cl}$ ,<sup>21</sup> and (c) the bent angle  $(\eta^3\text{-Ind})\text{-Mo}\text{-}(\eta^5\text{-Ind})$  of 130.4° in  $(\eta^3\text{-Ind})(\eta^5\text{-Ind})\text{-Mo}(\text{dppe})$ .<sup>22</sup> In general, the observed values for the ring-slippage parameters are typical for  $\eta^5$  coordination (**1**) and for  $\eta^3$  coordination (**13**) and are consistent with those given in the literature.<sup>13b,23,24</sup> The slip-fold angle  $\Omega$  of complex **13** (25.0°) is somewhat bigger than that for  $\text{IndCpMo}(\text{CO})_2$  (21.4°), probably reflecting its higher electron density at the metal.<sup>13</sup>

(21) Abugideiri, F.; Fetting, J. C.; Keogh, D. W.; and Poli, R. *Organometallics* **1996**, 15, 4407 and references therein.

(22) Poli, R.; Mattamiana, S. P.; and Falvello, L. R. *Gazz. Chim. Ital.* **1992**, 122, 315 and references therein.

(23) Faller, J. W.; Crabtree, R. H.; Habib, A. *Organometallics* **1985**, 4, 929.

(24) Ascenso, J. R.; Gonçalves, I. S.; Herdtweck, E.; Romão, C. C. *J. Organomet. Chem.* **1996**, 508, 169.

(25) Bocarsly, J. R.; Floriani, C.; Chiesi-Villa, A.; Guastini, C. *Inorg. Chem.* **1987**, 26, 1871 and references therein.

(26) Nesmeyanov, A. N.; Ustynuk, N. A.; Makarova, L. G.; Andrianov, V. G.; Struchkov, Yu. T.; Andrae, S. *J. Organomet. Chem.* **1978**, 159, 189.

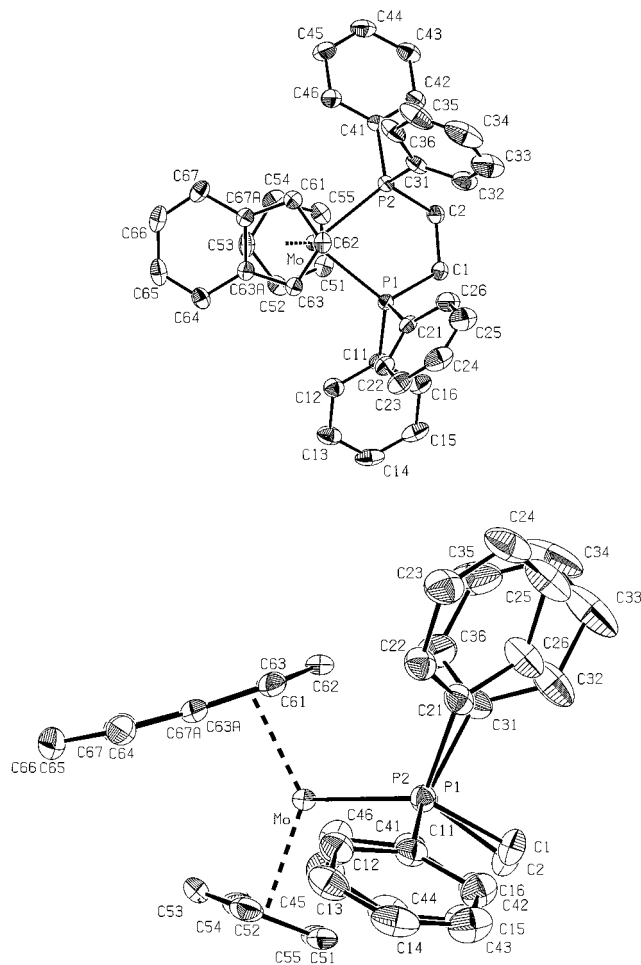


**Figure 2.** ORTEP style plots of the dication  $[(\eta^5\text{-Ind})(\text{Cp})\text{Mo}(\text{dppe})]^{2+}$  (**1**) with the atomic labeling scheme: (a, top) top view; (b, bottom) side view. Thermal ellipsoids are drawn at the 50% probability level. Hydrogen atoms are omitted for clarity.

Complex **1** presents a singular structural feature: it does not show the alignment of the indenyl ligand observed for  $[\text{IndCpMo}(\text{CO})(\text{NCMe})]^{2+}$ ,<sup>13</sup> as well as for all other structurally characterized  $\text{IndCpM}^{\text{IV}}$  complexes (*M* = Mo, W) and  $[\text{Ind}_2\text{V}(\text{CO})_2]^{2+}$ .<sup>25</sup> On the other hand, complex **13** shows a vector bisecting both the indenyl group and the L–M–L angle, as observed in the cases of  $\text{IndCpMo}(\text{CO})_2$ ,<sup>13</sup>  $\text{Ind}_2\text{W}(\text{CO})_2$ ,<sup>26</sup> and  $\text{Ind}_2\text{V}(\text{CO})_2$ .<sup>9b</sup>

## Discussion

Redox-induced ring slippage of the indenyl ligand between  $\eta^5$  and  $\eta^3$  coordination modes seems to be a quite general property in the modified molybdenocene complexes, according to eq 1.

As a matter of fact, this reversible chemical and electrochemical transformation was shown to occur for a variety of *L*<sub>2</sub> ligands (CO, CNR, PR<sub>3</sub>, bipyridyl). In the case of *L*<sub>2</sub> = dppe it was possible to characterize structurally the complexes at both ends of the redox pair, namely **1** and **13**, thereby confirming the haptotropic shift of the indenyl ligand. This is one of the few examples where such characterization is possible, the other ones being those described by Elschenbroich,<sup>1</sup> Geiger,<sup>6</sup> Sweigart,<sup>11</sup> Floriani,<sup>25</sup> and ourselves  $[(\text{IndCpMo}\{\text{P}(\text{OMe})_3\}_2]^{2+/0}$ .<sup>15</sup> Without this shift such a reduction is not possible or is totally irreversible, as we have shown for  $[\text{Cp}_2\text{Mo}(\text{dppe})]^{2+}$ .



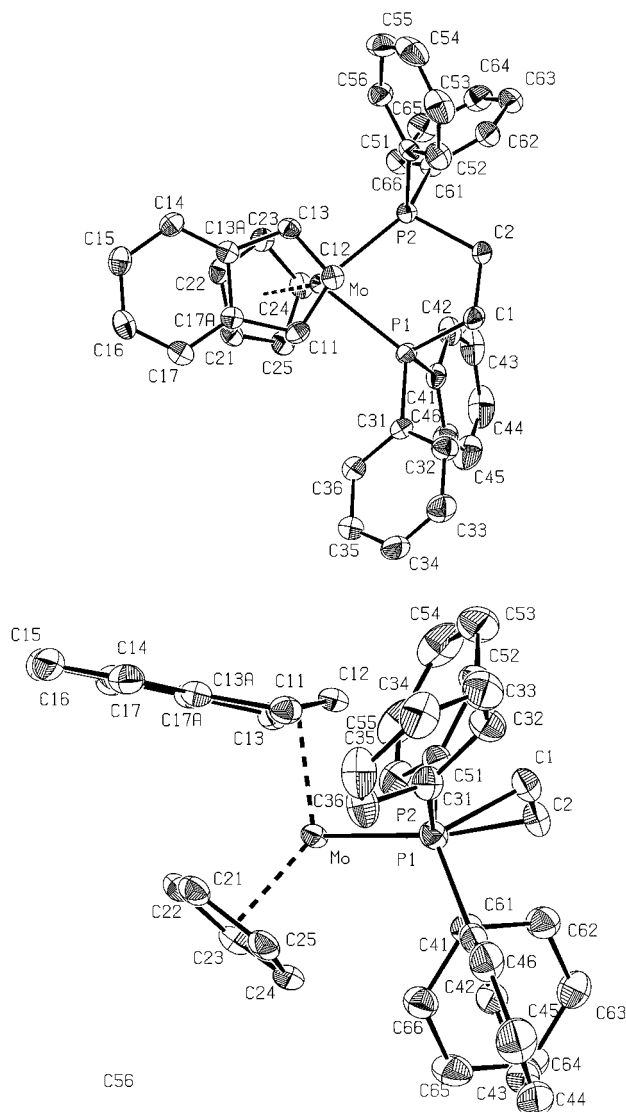
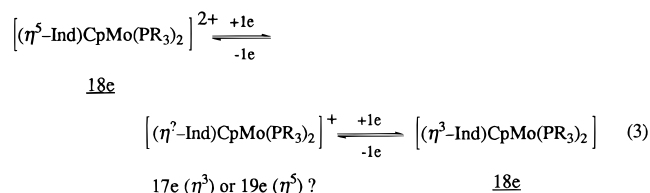


**Figure 3.** ORTEP style plots of  $[(\eta^3\text{-Ind})(\text{Cp})\text{Mo}(\text{dppe})]$  (**13**) with the atomic labeling scheme: (a, top) top view; (b, bottom) side view. Thermal ellipsoids are drawn at the 50% probability level. Hydrogen atoms are omitted for clarity.

The potential at which the electrochemical transformations take place is dependent on the nature of the ligands *L*. This is apparent not only from the value of these potentials but also from the resolution of the two one-electron transfers. Better  $\sigma$  donor and weaker  $\pi$  acceptor ligands *L* shift the potentials to more negative values. However, for all ligands tested except phosphines and  $\text{H}_2\text{biim}$ , the two 1e transfers are not resolved and a single 2e wave is recorded. In the case of the phosphines, two separated 1e waves are observed which correspond to the two one-electron-transfer steps in eq 3.



The intermediate monocations in eq 3 are stable within the CV time scale and are the first experimental

evidence for a group 6 bent metallocene in the formal +3 oxidation state. So far, only  $[\text{CpCp}'\text{MoL}_n]^{x+}$  complexes ( $M = \text{Cr}, \text{Mo}, \text{W}$ ;  $\text{Cp}' = \text{Cp}, \text{Ind}, \text{Cp}^*$ ) in the +2, +4, +5, and +6 oxidation states have been isolated and/or spectroscopically or electrochemically observed. This means that  $\text{PR}_3$  ligands are effective in stabilizing this intermediate odd-electron species. The separation between the waves is 150 mV for **1** and 280 mV for **2**. As argued by Cooper,<sup>10</sup> these small potential differences suggest marked stabilization of the final reduction products (**13** and **14**) by an  $\eta^5 \rightarrow \eta^3$  hapticity shift concomitant with the second reduction and also supports  $\eta^5$ -indenyl ligation in the first reduction product  $[(\eta^3\text{-Ind})\text{CpMo}(\text{PR}_3)_2]^+$ .

In the absence of their structural and/or spectroscopical characterization the actual hapticity of the indenyl ligand in these complexes remains unknown, and the fact that they are isoelectronic with the 17e  $[(\eta^3\text{-Ind})(\eta^5\text{-Ind})\text{V}(\text{CO})_2]$  is not compelling evidence in favor of a 17e  $[(\eta^3\text{-Ind})\text{CpMo}(\text{PR}_3)_2]^+$ .

To be able to answer this question, we are presently attempting the isolation of these and related complexes as well as promoting detailed theoretical and electrochemical studies on these redox-induced ring-slippage transformations.

## Experimental Section

All experiments were carried out under an atmosphere of nitrogen by Schlenk techniques. Diethyl ether, THF, and pentane were dried by distillation from Na/benzophenone. Acetonitrile was dried over  $\text{CaH}_2$  and distilled after refluxing several hours over  $\text{CaH}_2$  or  $\text{P}_2\text{O}_5$ . Dichloromethane was distilled from  $\text{CaH}_2$ . Acetone was distilled and kept over 4 Å molecular sieves.

Microanalyses and cyclic voltammetric measurements were performed in our laboratories (ITQB).  $^1\text{H}$  NMR spectra were obtained with a Bruker AMX 300 spectrometer. Infrared spectra were recorded on a Perkin-Elmer 457 and on a Unicam Mattson Mod 7000 FTIR spectrophotometer using KBr pellets.

$\text{PMe}_3$ ,<sup>27</sup>  $\text{H}_2\text{biim}$ ,<sup>28</sup>  $\text{CNMe}$ ,<sup>29</sup>  $[\text{IndCpMo}(\text{CO})_2][\text{BF}_4]_2$ ,  $[\text{IndCpMo}(\text{NCMe})_2][\text{BF}_4]_2$ ,  $[\text{IndCpMo}(\text{NCMe})\text{Cl}][\text{BF}_4]$ , and  $\text{IndCpMoCl}_2$ <sup>13</sup> were prepared as described previously.

**Electrochemistry.** The electrochemical instrumentation consisted of a BAS CV – 50W – 1000 Voltammetric Analyzer connected to BAS/Windows data acquisition software. All the electrochemical experiments were run under argon at room temperature. Tetrabutylammonium hexafluorophosphate (Aldrich) was used as supporting electrolyte; it was recrystallized from ethanol. Cyclic voltammetry experiments were performed in an MF-1082 glass cell from BAS in a C-2 cell enclosed in a Faraday cage. The reference electrode was SSC (MF-2063 from BAS), and its potential was – 44 mV relative to a SCE. The reference electrode was calibrated with a solution of ferrocene (1 mM) to obtain a potential in agreement with the literature value.<sup>30</sup>

The auxiliary electrode was a 7.5 cm platinum wire (MW-1032 from BAS) with a gold-plated connector. The working electrode was a platinum disk (MF-2013 from BAS) with ca. 0.022 cm<sup>2</sup> sealed in Kel-F plastic. Between each CV scan the working electrode was electrocleaned as a routine procedure and it was polished on 1  $\mu\text{M}$  diamond and subjected to alumina cleaning with water/methanol and sonicated, according to

(27) Wollsbarger, W.; Schmidbauer, H. *Synth. React. Inorg. Met.-Org. Chem.* **1974**, 4, 149.

(28) Calhorda, M. J.; Dias, A. R. *J. Organomet. Chem.* **1980**, 197, 291.

(29) Trofimenko, S. *J. Am. Chem. Soc.* **1967**, 89, 3170.

(30) Nelson, I. V.; Iwamoto, R. T. *Anal. Chem.* **1963**, 35, 867.

standard procedures, when necessary. Solvents were dried as previously described.

**Preparation of  $[\text{IndCpMo}(\text{dppe})][\text{BF}_4]_2$  (1). Method a.** A suspension of  $[\text{IndCpMo}(\text{NCMe})_2][\text{BF}_4]_2$  (0.31 g, 0.58 mmol) in  $\text{Me}_2\text{CO}$  was allowed to react with dppe (0.23 g, 0.58 mmol) for 5 h at room temperature. The supernatant red solution was filtered, and the remaining precipitate was further extracted with the reaction solvent. Upon concentration and cooling of the  $\text{Me}_2\text{CO}$  extracts, the salmon microcrystalline complex separated. It was washed with  $\text{CH}_2\text{Cl}_2$ , and red crystals were obtained by slow diffusion of  $\text{Et}_2\text{O}$  into a concentrated NCMe solution. Yield: 70%.

**Method b.** A solution of  $[\text{IndCpMo}(\text{NCMe})\text{Cl}][\text{BF}_4]$  (0.22 g, 0.50 mmol) in  $\text{Me}_2\text{CO}$  was treated with dppe (0.20 g, 0.50 mmol) and  $\text{TIBF}_4$  (0.20 g, 0.69 mmol), and this mixture was refluxed for 1 h. The supernatant solution was filtered, and the remaining precipitate was further extracted with  $\text{Me}_2\text{CO}$  ( $3 \times 20$  mL). The combined extracts were evaporated under vacuum, and the salmon powder so obtained was washed with  $\text{CH}_2\text{Cl}_2$  until the washings were colorless and recrystallized from NCMe/ $\text{Et}_2\text{O}$  in 40% yield.

**Method c.** A solution of  $(\eta^3\text{-Ind})\text{CpMo}(\text{dppe})$  (0.05 g, 0.08 mmol) in  $\text{CH}_2\text{Cl}_2$  was treated with a solution of  $\text{Ph}_3\text{CBF}_4$  (0.05 g, 0.15 mmol) in the same solvent. The reaction mixture became turbid, and after 3 h of stirring at room temperature the salmon precipitate was filtered off and washed with  $\text{CH}_2\text{Cl}_2$ . Yield: 80%.

Anal. Found: C, 56.63; H, 4.26. Calcd for  $\text{C}_{40}\text{H}_{36}\text{B}_2\text{F}_8\text{P}_2\text{Mo}$ : C, 56.64, H, 4.28%. Selected IR (KBr,  $\text{cm}^{-1}$ ):  $\nu$  3113, 3063, 1483, 1435, 1073, 830, 752, 698.  $^1\text{H}$  NMR ( $\text{CH}_3\text{CN}-d_3$ , 300 MHz, room temp,  $\delta$  (ppm)): 7.64–7.13 (c, 22H, Ph +  $\text{H}^{5-8}$ ); 6.65–6.62 (m, 2H,  $\text{H}^{5-8}$ ); 6.28–6.26 (m, 1H,  $\text{H}^2$ ); 5.56–5.53 (m, 2H,  $\text{H}^{1/3}$ ); 5.08 (t, 5H, Cp, [ $^3J_{\text{PH}} = 2.2$  Hz]); 3.62–3.20 (c, 4H,  $\text{CH}_2$  of dppe).  $^{13}\text{C}$  NMR ( $\text{CH}_3\text{CN}-d_3$ , 75 MHz, room temp,  $\delta$  (ppm)): 135.1 ( $\text{C}^{5/8}$ ); 133.4–130.8 (c, dppe); 127.3 ( $\text{C}^{6/7}$ ); 112.4 ( $\text{C}^{4/9}$ ); 99.2 (Cp); 89.2 ( $\text{C}^2$ ); 82.3 ( $\text{C}^{1/3}$ ); 28.5 (dppe).

**Reaction of  $[\text{IndCpMo}(\text{CO})_2][\text{BF}_4]_2$  with dppe.** A suspension of  $[\text{IndCpMo}(\text{CO})_2][\text{BF}_4]_2$  (0.35 g, 0.70 mmol) in  $\text{Me}_2\text{CO}$  was treated with dppe (0.28 g, 0.70 mmol), and this mixture was refluxed and irradiated with a 60 W tungsten bulb for 4 h. The solvent of the resulting yellow solution was evaporated under vacuum to yield a powder which was completely dissolved in  $\text{CH}_2\text{Cl}_2$ . After concentration to ca. 5 mL and addition of  $\text{Et}_2\text{O}$ ,  $[\text{CpMo}(\text{CO})_2(\text{dppe})][\text{BF}_4]$  precipitated as a yellow powder, in 80% yield. The complex was identified by comparison of its IR and  $^1\text{H}$  NMR spectra with those of an authentic sample.<sup>16</sup> Crystals were obtained from a slow  $\text{CH}_2\text{Cl}_2/\text{Et}_2\text{O}$  recrystallization.

Anal. Found: C, 56.04; H, 4.45. Calcd for  $\text{C}_{33}\text{H}_{29}\text{BF}_4\text{O}_2\text{P}_2\text{Mo}$ : C, 56.44, H, 4.16%. Selected IR (KBr,  $\text{cm}^{-1}$ ):  $\nu$  3055; 1975, 1906 (sv, CO); 1697; 1485; 1437; 1084; 746; 698.  $^1\text{H}$  NMR ( $\text{CH}_3\text{CN}-d_3$ , 300 MHz, room temp,  $\delta$  (ppm)): 7.61–7.43 (c, 20H, Ph); 4.75 (s (br), 5H, Cp); 2.93–2.85 (m, 2H,  $\text{CH}_2$  of dppe); 2.13–1.99 (m, 2H,  $\text{CH}_2$  of dppe).

**Preparation of  $[\text{IndCpMo}(\text{PMe}_3)_2][\text{BF}_4]_2$  (2). Method a.** A suspension of  $\text{IndCpMoCl}_2$  (0.25 g, 0.71 mmol) in  $\text{CH}_2\text{Cl}_2$  was treated with  $\text{PMe}_3$  (0.16 mL) and  $\text{TIBF}_4$  (0.41 g, 1.42 mmol). After the mixture was stirred for 12 h, the supernatant solution was filtered and the remaining precipitate was extracted with  $\text{Me}_2\text{CO}$  ( $3 \times 40$  mL). Upon concentration and cooling the pink microcrystalline complex separated. The complex was recrystallized from  $\text{Me}_2\text{CO}/\text{Et}_2\text{O}$  in 70% yield.

**Method b.** A solution of  $[\text{IndCpMo}(\text{NCMe})_2][\text{BF}_4]_2$  (0.19 g, 0.36 mmol) in  $\text{CH}_2\text{Cl}_2/\text{NMF}$  (10/1) was allowed to react with  $\text{PMe}_3$  (0.07 mL, 0.72 mmol) for 4 h at room temperature. The resulting red solution was concentrated under vacuum until the only remaining solvent was NMF. Addition of  $\text{Et}_2\text{O}/\text{EtOH}$  (30/1) allowed the precipitation of the pink product. This was washed with  $\text{CH}_2\text{Cl}_2$  and  $\text{Et}_2\text{O}$ .

Anal. Found: C, 24.78; H, 4.25; N, 3.97%. Calcd for  $\text{C}_{20}\text{H}_{30}\text{B}_2\text{F}_8\text{P}_2\text{Mo}$ : C, 25.03, H, 3.97%. Selected IR (KBr,  $\text{cm}^{-1}$ ):  $\nu$  3366, 3092,

2912, 1423, 1300, 1084, 965, 845, 779.  $^1\text{H}$  NMR ( $\text{CH}_3\text{CN}-d_3$ , 300 MHz, room temp,  $\delta$  (ppm)): 7.67 (s, 4H,  $\text{H}^{5-8}$ ); 6.00–5.97 (m, 2H,  $\text{H}^{1/3}$ ); 5.47–5.42 (m, 1H,  $\text{H}^2$ ); 5.10 (t, 5H, Cp, [ $^3J_{\text{PH}} = 2.1$  Hz]); 1.66–1.62 (t, 18H,  $\text{CH}_3$ ).  $^{13}\text{C}$  NMR ( $\text{CH}_3\text{CN}-d_3$ , 75 MHz, room temp,  $\delta$  (ppm)): 134.9 ( $\text{C}^{5/8}$ ); 127.0 ( $\text{C}^{6/7}$ ); 112.3 ( $\text{C}^{4/9}$ ); 97.4 (Cp); 91.6 ( $\text{C}^2$ ); 87.4 ( $\text{C}^{1/3}$ ); 21.1 ( $\text{PMe}_3$ ).

**Reaction of  $\text{IndCpMoCl}_2$  with  $\text{TIBF}_4$  and Excess  $\text{PMe}_3$  in Acetone To Afford  $[\text{CpMo}(\text{PMe}_3)_4]\text{BF}_4$  (3).** A suspension of  $\text{IndCpMoCl}_2$  (0.24 g, 0.70 mmol) in  $\text{Me}_2\text{CO}$  was treated with excess  $\text{PMe}_3$  (1.0 mL, 10 mmol) and  $\text{TIBF}_4$  (0.44 g, 1.5 mmol), and the mixture was stirred for 1 h at room temperature. The supernatant solution was separated from the  $\text{TiCl}_3$  precipitate by filtration and taken to dryness under vacuum. The residue was extracted with  $\text{CH}_2\text{Cl}_2$  and air-sensitive complex  $[\text{CpMo}(\text{PMe}_3)_4]\text{BF}_4$  obtained as a red powder upon evaporation of the solvent and washing with  $\text{Et}_2\text{O}$ . Yield: 40%.

Anal. Found: C, 24.78; H, 3.97. Calcd for  $\text{C}_{17}\text{H}_{14}\text{BF}_4\text{P}_4\text{Mo}$ : C, 25.03, H, 3.97. Selected IR (KBr,  $\text{cm}^{-1}$ ):  $\nu$  310, 2980, 2910, 1906, 1423, 1302, 1084, 966, 843.  $^1\text{H}$  NMR ( $\text{Me}_2\text{CO}-d_6$ , 300 MHz, room temp,  $\delta$  (ppm)): 5.66 (s (br), 5H, Cp); 1.88–1.70 (c, 36H,  $\text{CH}_3$ ).

**Preparation of  $[\text{IndCpMo}(\text{Bipy})][\text{BF}_4]_2$  (4).** A solution of  $[\text{IndCpMo}(\text{NCMe})_2][\text{BF}_4]_2$  (0.30 g, 0.56 mmol) in  $\text{CH}_2\text{Cl}_2/\text{NMF}$  (10/1) was allowed to react with 2,2'-bipyridyl (0.09 g, 0.56 mmol) for 2 h at room temperature. The resulting dark violet solution was concentrated under vacuum until the only remaining solvent was NMF. Addition of  $\text{Et}_2\text{O}/\text{EtOH}$  (30/1) allowed the precipitation of the violet product. This was recrystallized from  $\text{Me}_2\text{CO}/\text{Et}_2\text{O}$  in 60% yield.

Anal. Found: C, 47.67; H, 3.44; N, 4.46. Calcd for  $\text{C}_{24}\text{H}_{20}\text{B}_2\text{F}_8\text{N}_2\text{Mo}$ : C, 47.57, H, 3.33, N, 4.62. Selected IR (KBr,  $\text{cm}^{-1}$ ):  $\nu$  3399, 3063, 1601, 1442, 1100, 860, 789.  $^1\text{H}$  NMR ( $\text{Me}_2\text{CO}-d_6$ , 300 MHz, room temp,  $\delta$  (ppm)): 8.80 (d (br), 2H, Bipy); 8.50 (t (br), 2H, Bipy); 7.97 (d (br), 2H, Bipy); 7.69 (c, 4H, Bipy +  $\text{H}^{5-8}$ ); 7.35–7.32 (m, 2H,  $\text{H}^{5-8}$ ); 6.63 (t, 1H,  $\text{H}^2$ ); 6.34 (d, 2H,  $\text{H}^{1/3}$ ); 6.17 (s, 5H, Cp).  $^{13}\text{C}$  NMR ( $\text{CH}_3\text{CN}-d_3$ , 75 MHz, room temp,  $\delta$  (ppm)): 172.6 (Bipy); 158.2 (Bipy); 144.0 (Bipy); 135.2 ( $\text{C}^{5/8}$ ); 129.0 (Bipy); 128.2 (Bipy); 126.3 ( $\text{C}^{6/7}$ ); 116.2 ( $\text{C}^{4/9}$ ); 106.2 (Bipy); 105.6 (Bipy); 104.4 (Bipy); 103.6 (Cp); 96.9 (Bipy); 94.5 (Bipy); 93.6 ( $\text{C}^2$ ); 93.1 ( $\text{C}^{1/3}$ ); 27.1 (Bipy); 24.7 (Bipy).

**Preparation of  $[\text{IndCpMo}(\text{Bu}_2\text{bipy})][\text{BF}_4]_2$  (5).** A suspension of  $[\text{IndCpMo}(\text{NCMe})_2][\text{BF}_4]_2$  (0.37 g, 0.70 mmol) in  $\text{Me}_2\text{CO}$  was allowed to react with 4,4'-di-*tert*-butyl-2,2'-bipyridine (0.19 g, 0.70 mmol) for 1 h at room temperature. The violet solution was taken to dryness, and the resulting powder was recrystallized from  $\text{CH}_2\text{Cl}_2/\text{Et}_2\text{O}$  in quantitative yield.

Anal. Found: C, 53.05; H, 4.86; N, 4.00. Calcd for  $\text{C}_{32}\text{H}_{36}\text{B}_2\text{F}_8\text{N}_2\text{Mo}$ : C, 53.52, H, 5.05, N, 3.90. Selected IR (KBr,  $\text{cm}^{-1}$ ):  $\nu$  3121, 2967, 1618, 1543, 1483, 1415, 1369, 1252, 1060, 845, 768.  $^1\text{H}$  NMR ( $\text{Me}_2\text{CO}-d_6$ , 300 MHz, room temp,  $\delta$  (ppm)): 8.69 (s (br), 2H,  $\text{Bu}_2\text{bipy}$ ); 7.76 (d (br), 2H,  $\text{Bu}_2\text{bipy}$ ); 7.56 (m, 2H,  $\text{Bu}_2\text{bipy}$ ); 7.53–7.50 (m, 2H,  $\text{H}^{5-8}$ ); 7.19–7.16 (m, 2H,  $\text{H}^{5-8}$ ); 6.43 (t, 1H,  $\text{H}^2$ ); 6.14 (d, 2H,  $\text{H}^{1/3}$ ); 5.98 (s, 5H, Cp); 1.31 (s, 18H,  $\text{CH}_3$ ).

**Preparation of  $[\text{IndCpMo}(\text{H}_2\text{biim})][\text{BF}_4]_2$  (6).** A solution of  $[\text{IndCpMo}(\text{NCMe})_2][\text{BF}_4]_2$  (0.26 g, 0.50 mmol) in  $\text{CH}_2\text{Cl}_2/\text{NMF}$  (10/1) was allowed to react overnight with  $\text{H}_2\text{biim}$  (0.07 g, 0.50 mmol) under reflux. Upon concentration under vacuum (until the only remaining solvent was NMF) followed by the addition of  $\text{Et}_2\text{O}$ , the violet microcrystalline complex separated. The compound was washed with  $\text{CH}_2\text{Cl}_2$ . Yield: 90%.

Anal. Found: C, 41.15; H, 3.24; N, 9.12. Calcd for  $\text{C}_{20}\text{H}_{18}\text{B}_2\text{F}_8\text{N}_4\text{Mo}$ : C, 41.14, H, 3.11, N, 9.59. Selected IR (KBr,  $\text{cm}^{-1}$ ):  $\nu$  3370, 3086, 1665, 1535, 1495, 1427, 1072, 842, 762.  $^1\text{H}$  NMR ( $\text{Me}_2\text{CO}-d_6$ , 300 MHz, room temp,  $\delta$  (ppm)): 8.11 (s (br), 2H, N–H); 7.66 (d, 2H,  $\text{H}_2\text{biim}$ ); 7.59–7.55 (m, 2H,  $\text{H}^{5-8}$ ); 7.44–7.41 (m, 2H,  $\text{H}^{5-8}$ ); 6.99 (d, 2H,  $\text{H}_2\text{biim}$ ); 6.57 (t, 1H,  $\text{H}^2$ ); 6.20 (d, 2H,  $\text{H}^{1/3}$ ); 5.91 (s, 5H, Cp).  $^{13}\text{C}$  NMR ( $\text{CH}_3\text{CN}-d_3$ , 75 MHz, room temp,  $\delta$  (ppm)): 143.6 ( $\text{H}_2\text{biim}$ ); 133.9 ( $\text{C}^{5/8}$ ); 133.1 ( $\text{H}_2$ –



biim); 127.9 (C<sup>6/7</sup>); 123.5 (C<sup>4/9</sup>); 101.9 (Cp); 92.6 (C<sup>2</sup>); 91.7 (C<sup>1/3</sup>); 25.2 (H<sub>2</sub>biim).

**Preparation of [IndCpMo(CO)(CNMe)<sub>2</sub>][BF<sub>4</sub>]<sub>2</sub> (7).** A suspension of [IndCpMo(CO)<sub>2</sub>][BF<sub>4</sub>]<sub>2</sub> (0.35 g, 0.70 mmol) in CH<sub>2</sub>Cl<sub>2</sub> was treated with excess CNMe (200  $\mu$ L), and the reaction mixture was refluxed and irradiated with a 60 W tungsten bulb for 10 h. The supernatant solution was filtered and the precipitate washed with CH<sub>2</sub>Cl<sub>2</sub>. The dark yellow complex was recrystallized from NCMe/Et<sub>2</sub>O in 80% yield.

Anal. Found: C, 39.32; H, 2.83; N, 3.19. Calcd for C<sub>17</sub>H<sub>15</sub>B<sub>2</sub>F<sub>8</sub>NOMo: C, 39.35, H, 2.91, N, 2.70. Selected IR (KBr, cm<sup>-1</sup>):  $\nu$  3079; 2255, 2076 (sv, CO); 1537; 1447; 1416; 1300; 1119; 871; 766. <sup>1</sup>H NMR (CH<sub>3</sub>CN-*d*<sub>3</sub>, 300 MHz, room temp,  $\delta$  (ppm)): 7.88–7.76 (m, 4H, H<sup>5-8</sup>); 6.72–6.68 (c, 2H, H<sup>1/3</sup>); 6.32 (t, 1H, H<sup>2</sup>); 6.03 (s, 5H, Cp); 3.57 (s, 3H, CH<sub>3</sub>).

**Preparation of [IndCpMo(CNMe)<sub>2</sub>][BF<sub>4</sub>]<sub>2</sub> (8). Method a.** A suspension of [IndCpMo(CO)<sub>2</sub>][BF<sub>4</sub>]<sub>2</sub> (0.35 g, 0.70 mmol) in CH<sub>2</sub>Cl<sub>2</sub> was treated with a large excess of CNMe (400  $\mu$ L) and the reaction mixture refluxed and irradiated with a 60 W tungsten bulb for 24 h. The supernatant solution was filtered and the precipitate washed with Me<sub>2</sub>CO. The yellow complex was recrystallized from NCMe/Et<sub>2</sub>O in 40% yield.

**Method b.** Addition of excess CNMe (300  $\mu$ L) to a solution of [IndCpMo(NCMe)<sub>2</sub>][BF<sub>4</sub>]<sub>2</sub> (0.30 g, 0.56 mmol) in CH<sub>2</sub>Cl<sub>2</sub>/NMF (10/1) caused an immediate change of color from violet to yellow. After 1 h of stirring at room temperature, the solution was concentrated under vacuum (until the only remaining solvent was NMF) and Et<sub>2</sub>O/EtOH (30/1) added to precipitate the yellow complex. The compound was washed with CH<sub>2</sub>Cl<sub>2</sub>. Yield: 90%.

Anal. Found: C, 40.61; H, 3.39; N, 5.15. Calcd for C<sub>18</sub>H<sub>18</sub>B<sub>2</sub>F<sub>8</sub>N<sub>2</sub>Mo: C, 40.65, H, 3.41, N, 5.27. Selected IR (KBr, cm<sup>-1</sup>):  $\nu$  3102, 2245, 1537, 1447, 1414, 1304, 1084, 866, 770. <sup>1</sup>H NMR (CH<sub>3</sub>CN-*d*<sub>3</sub>, 300 MHz, room temp,  $\delta$  (ppm)): 7.71–7.68 (m, 4H, H<sup>5-8</sup>); 6.34 (d, 2H, H<sup>1/3</sup>); 6.05 (t, 1H, H<sup>2</sup>); 5.70 (s, 5H, Cp); 3.59 (s, 6H, CH<sub>3</sub>). <sup>13</sup>C NMR (CH<sub>3</sub>CN-*d*<sub>3</sub>, 75 MHz, room temp,  $\delta$  (ppm)): 141.7 (CNMe); 134.7 (C<sup>5/8</sup>); 127.3 (C<sup>6/7</sup>); 112.8 (C<sup>4/9</sup>); 98.1 (Cp); 89.7 (C<sup>2</sup>); 89.3 (C<sup>1/3</sup>); 32.9 (CNCH<sub>3</sub>).

**Preparation of [IndCpMo(CNCMe)<sub>2</sub>][BF<sub>4</sub>]<sub>2</sub> (9).** Addition of excess CN<sup>t</sup>Bu (0.20 mL) to a solution of [IndCpMo(NCMe)<sub>2</sub>][BF<sub>4</sub>]<sub>2</sub> (0.30 g, 0.56 mmol) in CH<sub>2</sub>Cl<sub>2</sub>/NMF (10/1) caused an immediate change of color from violet to light yellow. After 1 h of stirring at room temperature, the solution was concentrated under vacuum (until the only remaining solvent was NMF) and Et<sub>2</sub>O/EtOH (30/1) added to precipitate the yellow complex. The compound was washed with CH<sub>2</sub>Cl<sub>2</sub>. Yield: 95%.

Anal. Found: C, 46.79; H, 4.79; N, 4.56. Calcd for C<sub>24</sub>H<sub>30</sub>B<sub>2</sub>F<sub>8</sub>N<sub>2</sub>Mo: C, 46.79, H, 4.91, N, 4.55. Selected IR (KBr, cm<sup>-1</sup>):  $\nu$  3320, 3055, 2978, 2220, 2200, 1464, 1373, 1200, 1072, 876, 766. <sup>1</sup>H NMR (Me<sub>2</sub>CO-*d*<sub>6</sub>, 300 MHz, room temp,  $\delta$  (ppm)): 8.00–7.98 (m, 2H, H<sup>5-8</sup>); 7.84–7.81 (m, 2H, H<sup>5-8</sup>); 6.81 (d, 2H, H<sup>1/3</sup>); 6.37 (t, 1H, H<sup>2</sup>); 6.11 (s, 5H, Cp); 1.66 (s, 18H, CH<sub>3</sub>). <sup>13</sup>C NMR (CH<sub>3</sub>CN-*d*<sub>3</sub>, 75 MHz, room temp,  $\delta$  (ppm)): 142.3 (CNCMe<sub>3</sub>); 134.8 (C<sup>5/8</sup>); 127.3 (C<sup>6/7</sup>); 112.7 (C<sup>4/9</sup>); 98.4 (Cp); 89.6 (C<sup>2</sup>); 89.3 (C<sup>1/3</sup>); 62.8 (CNCMe<sub>3</sub>); 29.7 (CNC(CH<sub>3</sub>)<sub>3</sub>).

**Preparation of [IndCpMo(NCMe)(NMF)][BF<sub>4</sub>]<sub>2</sub> (10).** A solution of [IndCpMo(NCMe)<sub>2</sub>][BF<sub>4</sub>]<sub>2</sub> (0.25 g, 0.47 mmol) in CH<sub>2</sub>Cl<sub>2</sub>/NMF (10/1) was stirred for 3 h at room temperature. The resulting dark violet solution was concentrated under vacuum until the only remaining solvent was NMF. Addition of Et<sub>2</sub>O/EtOH (30/1) allowed the precipitation of the violet product. This was washed with CH<sub>2</sub>Cl<sub>2</sub> and Et<sub>2</sub>O.

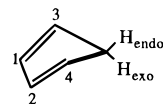
Anal. Found: C, 39.50; H, 3.49; N, 5.11. Calcd for C<sub>18</sub>H<sub>20</sub>B<sub>2</sub>F<sub>8</sub>N<sub>2</sub>OMo: C, 39.31; H, 3.67; N, 5.09. Selected IR (KBr, cm<sup>-1</sup>):  $\nu$  3233, 3052, 2292, 1643, 1421, 1350, 1068, 852, 756. <sup>1</sup>H NMR (Me<sub>2</sub>CO-*d*<sub>6</sub>, 300 MHz, room temp,  $\delta$  (ppm)): 7.91–7.88 (m, 2H, H<sup>5-8</sup>); 7.74–7.71 (m, 2H, H<sup>5-8</sup>); 6.71 (d, 2H, H<sup>1/3</sup>); 6.65 (t, 1H, H<sup>2</sup>); 6.19 (s, 5H, Cp); 2.83 (s, 3H, CH<sub>3</sub>); 2.63 (s, 3H, NCMe).

**Preparation of [IndCpMo(NMF)<sub>2</sub>][BF<sub>4</sub>]<sub>2</sub> (11).** A solution of [IndCpMo(NCMe)<sub>2</sub>][BF<sub>4</sub>]<sub>2</sub> (0.25 g, 0.47 mmol) in CH<sub>2</sub>Cl<sub>2</sub>/NMF (10/1) was refluxed overnight. The resulting dark green solution was concentrated under vacuum until the only remaining solvent was NMF. Addition of Et<sub>2</sub>O/EtOH (30/1) allowed the precipitation of the green product. This was washed with CH<sub>2</sub>Cl<sub>2</sub> and Et<sub>2</sub>O.

Anal. Found: C, 38.16; H, 3.93; N, 4.83. Calcd for C<sub>18</sub>H<sub>22</sub>B<sub>2</sub>F<sub>8</sub>N<sub>2</sub>O<sub>2</sub>Mo: C, 38.07; H, 3.90; N, 4.93. Selected IR (KBr, cm<sup>-1</sup>):  $\nu$  3230, 3052, 1640, 1432, 1350, 1072, 852, 756. <sup>1</sup>H NMR (Me<sub>2</sub>CO-*d*<sub>6</sub>, 300 MHz, room temp,  $\delta$  (ppm)): 7.66 (s (br), 2H, H<sup>5-8</sup>); 7.60 (s (br), 2H, H<sup>5-8</sup>); 6.53 (t, 1H, H<sup>2</sup>); 6.46 (d, 2H, H<sup>1/3</sup>); 6.19 (s, 5H, Cp); 3.74 (s, 6H, CH<sub>3</sub>).

**Preparation of [IndMo( $\eta^4$ -C<sub>5</sub>H<sub>6</sub>)(dppe)][BF<sub>4</sub>]<sub>2</sub>·CH<sub>2</sub>Cl<sub>2</sub> (12).** Addition of NaBH<sub>4</sub> (7.2 mg, 0.19 mmol) to a solution of [IndCpMo(dppe)][BF<sub>4</sub>]<sub>2</sub> (0.14 g, 0.16 mmol) in Me<sub>2</sub>CO caused an immediate change of color from salmon to dark orange. After it was stirred for 1 h at room temperature, the reaction mixture was taken to dryness and the residue was extracted with CH<sub>2</sub>Cl<sub>2</sub> to give the dark brick red complex in quantitative yield.

Anal. Found: C, 58.15; H, 4.86. Calcd for C<sub>41</sub>H<sub>39</sub>BF<sub>4</sub>Cl<sub>2</sub>P<sub>2</sub>Mo: C, 58.12, H, 4.64. Selected IR (KBr, cm<sup>-1</sup>):  $\nu$  3053, 2970, 2768, 1697, 1483, 1435, 1084, 748, 698. <sup>1</sup>H NMR (CH<sub>2</sub>Cl<sub>2</sub>-*d*<sub>2</sub>, 300 MHz, room temp,  $\delta$  (ppm)): 7.42–6.81 (c, 24H, Ph + H<sup>5-8</sup>); 6.50 (m, 2H, H<sup>1/3</sup>); 4.99 (t, 1H, H<sup>2</sup>); 4.27 (s (br), 2H, H<sub>1-2</sub>); 3.49 (s (br), 2H, H<sub>3-4</sub>); 3.32 (s (br), 1H, H<sub>exo</sub>); 2.85 (s (br), 1H, H<sub>endo</sub>); 2.06 (s, 4H, CH<sub>2</sub> of dppe).



**Preparation of ( $\eta^3$ -Ind)CpMo(dppe) (13). Method a.** A solution of [IndMo( $\eta^4$ -C<sub>5</sub>H<sub>6</sub>)(dppe)][BF<sub>4</sub>]<sub>2</sub> (0.34 g, 0.50 mmol) in CH<sub>2</sub>Cl<sub>2</sub> was treated with excess NEt<sub>3</sub> (0.5 mL). After the mixture was stirred for 2 h at room temperature, the solvent of the orange solution was removed under vacuum and the residue extracted with toluene (3  $\times$  30 mL). The orange powder obtained upon concentration of the extract was washed with cold pentane. Yield: 50%.

**Method b.** The addition of an NCMe solution of Cp<sub>2</sub>Co (0.18 g, 0.95 mmol) to the complex [IndCpMo(dppe)][BF<sub>4</sub>]<sub>2</sub> (0.40 g, 0.48 mmol) dissolved in the same solvent caused an immediate change in color from salmon to orange together with the appearance of a precipitate. After the mixture was stirred for 2 h at room temperature, the solvent was removed under vacuum and the residue extracted with toluene. Upon concentration and cooling of the extract the orange microcrystalline product separated in 95% yield.

Anal. Found: C, 71.39; H, 5.21. Calcd for C<sub>40</sub>H<sub>36</sub>P<sub>2</sub>Mo: C, 71.22, H, 5.38. Selected IR (KBr, cm<sup>-1</sup>):  $\nu$  3048, 1481, 1433, 1302, 1202, 1092, 1009, 922, 820, 740, 696. <sup>1</sup>H NMR (C<sub>6</sub>H<sub>6</sub>-*d*<sub>6</sub>, 300 MHz, room temp,  $\delta$  (ppm)): 7.42–6.88 (c, 20H, Ph); 6.46 (d, 4H, H<sup>5-8</sup>); 4.48 (s (br), 5H, Cp); 2.96 (s (br), 3H, H<sup>1/3</sup>); 2.17–1.83 (c, 4H, CH<sub>2</sub> of dppe). <sup>13</sup>C NMR (CH<sub>2</sub>Cl<sub>2</sub>-*d*<sub>2</sub>, 75 MHz, room temp,  $\delta$  (ppm)): 151.5 (C<sup>4/9</sup>); 133.4–129.1 (c, dppe + C<sup>5/8</sup>); 118.0 (C<sup>6/7</sup>); 114.2 (C<sup>2</sup>); 86.2 (Cp); 64.99 (C<sup>1/3</sup>); 29.6 (dppe).

**Preparation of ( $\eta^3$ -Ind)CpMo(PMe<sub>3</sub>)<sub>2</sub> (14).** The addition of an NCMe solution of Cp<sub>2</sub>Co (0.24 g, 1.30 mmol) to the complex [IndCpMo(PMe<sub>3</sub>)<sub>2</sub>][BF<sub>4</sub>]<sub>2</sub> (0.39 g, 0.65 mmol) dissolved in the same solvent caused an immediate change of color from violet to orange together with the appearance of a fine precipitate. After the mixture was stirred for 1 h at room temperature, the solvent was removed under vacuum and the residue extracted with warm Et<sub>2</sub>O (3  $\times$  30 mL). Upon concentration and cooling of the extract the orange microcrystalline product separated in 50% yield.

Anal. Found: C, 56.42; H, 7.39. Calcd for C<sub>20</sub>H<sub>30</sub>P<sub>2</sub>Mo: C, 56.42, H, 5.39. MS (EI; *m/z*): 430 (M<sup>+</sup>); 354 (M<sup>+</sup> – PMe<sub>3</sub>); 278

(M<sup>+</sup> – 2PMe<sub>3</sub>); 116 (IndH<sup>+</sup>). Selected IR (KBr, cm<sup>-1</sup>):  $\nu$  3100, 2920, 1416, 1263, 866, 806. <sup>1</sup>H NMR (C<sub>6</sub>H<sub>6</sub>-d<sub>6</sub>, 300 MHz, room temp,  $\delta$  (ppm)): 6.52 (s (br), 4H, H<sup>5-8</sup>); 6.26 (s (br), 1H, H<sup>2</sup>); 4.17 (s (br), 5H, Cp); 3.03 (s (br), 3H, H<sup>1/3</sup>); 0.68 (t (br), 18H, PMe<sub>3</sub>).

**Preparation of ( $\eta^3$ -Ind)CpMo(Bipy) (15).** The addition of an NCMe solution of Cp<sub>2</sub>Co (0.24 g, 1.30 mmol) to the complex [IndCpMo(Bipy)<sub>2</sub>][BF<sub>4</sub>]<sub>2</sub> (0.23 g, 0.39 mmol) dissolved in the same solvent caused an immediate change in color from violet to deep purple. After the mixture was stirred for 1 h at room temperature, the solvent was removed under vacuum and the residue extracted with a hexane/ether mixture (1/1) (2  $\times$  30 mL). Upon concentration and cooling of the extract the deep purple microcrystalline product separated in 90% yield.

Anal. Found: C, 67.09; H, 5.04; N, 6.97. Calcd for C<sub>24</sub>H<sub>20</sub>N<sub>2</sub>-Mo: C, 66.67, H, 4.66, N, 6.48. Selected IR (KBr, cm<sup>-1</sup>):  $\nu$  3048, 2928, 1450, 1294, 1240, 1153, 995, 826, 760. <sup>1</sup>H NMR (C<sub>6</sub>H<sub>6</sub>-d<sub>6</sub>, 300 MHz, room temp,  $\delta$  (ppm)): 8.54 (d, 2H, Bipy); 7.33 (d, 2H, Bipy); 6.78 (m, 2H, H<sup>5-8</sup>); 6.68 (m, 2H, H<sup>5-8</sup>); 6.47 (t, 2H, Bipy); 5.96 (t, 2H, Bipy); 4.77 (d, 2H, H<sup>1/3</sup>); 4.36 (s, 5H, Cp); 3.44 (s (br), 1H, H<sup>2</sup>).

**Preparation of ( $\eta^3$ -Ind)CpMo(CO)(CNMe) (16).** A toluene solution of Cp<sub>2</sub>Co (0.06 g, 0.33 mmol) was added to the complex [IndCpMo(CO)(CNMe)][BF<sub>4</sub>]<sub>2</sub> (0.08 g, 0.16 mmol) suspended in the same solvent. After the mixture was stirred for 2 h at room temperature, the solvent was removed under vacuum and the residue extracted with hexane (2  $\times$  30 mL). Upon concentration and cooling of the extract the brick red microcrystalline product separated in 80% yield.

Anal. Found: C, 59.35; H, 3.90; N, 4.42. Calcd for C<sub>17</sub>H<sub>15</sub>-NOMo: C, 59.14, H, 4.38, N, 4.06. Selected IR (KBr, cm<sup>-1</sup>):  $\nu$  3106, 2131, 1863, 1415, 1201, 1010, 871. <sup>1</sup>H NMR (C<sub>6</sub>H<sub>6</sub>-d<sub>6</sub>, 300 MHz, room temp,  $\delta$  (ppm)): 7.16 (s (br), 1H, H<sup>5-8</sup>); 6.88 (t, 1H, H<sup>5-8</sup>); 6.65 (s (br), 1H, H<sup>5-8</sup>); 6.51 (t, 1H, H<sup>5-8</sup>); 5.50 (m, 1H, H<sup>2</sup>); 4.85 (t, 1H, H<sup>1/3</sup>); 4.69 (s, 5H, Cp); 4.62 (t, 1H, H<sup>1/3</sup>); 2.18 (s, 3H, CH<sub>3</sub>).

**Preparation of ( $\eta^3$ -Ind)CpMo(CNCMe<sub>3</sub>)<sub>2</sub> (17).** Addition of a fresh NCMe solution of Cp<sub>2</sub>Co (0.11 g, 0.59 mmol) to the complex [IndCpMo(CNCMe<sub>3</sub>)<sub>2</sub>][BF<sub>4</sub>]<sub>2</sub> (0.26 g, 0.30 mmol) dissolved in the same solvent caused an immediate reaction. After the mixture was stirred for 1 h at room temperature, the solvent was removed under vacuum and the residue extracted with hexane (2  $\times$  30 mL). Upon concentration and cooling of the extract the yellow complex separated as a powder, in 50% yield.

Anal. Found: C, 65.59; H, 6.33; N, 5.98. Calcd for C<sub>24</sub>H<sub>30</sub>N<sub>2</sub>-Mo: C, 65.15, H, 6.83, N, 6.33. Selected IR (KBr, cm<sup>-1</sup>):  $\nu$  3055, 2978, 2081, 2047, 1456, 1200, 1033, 793, 746. <sup>1</sup>H NMR (C<sub>6</sub>H<sub>6</sub>-d<sub>6</sub>, 300 MHz, room temp,  $\delta$  (ppm)): 6.81 (t, 1H, H<sup>2</sup>); 6.64–6.61 (m, 2H, H<sup>5-8</sup>); 6.51–6.48 (m, 2H, H<sup>5-8</sup>); 4.80 (s, 5H, Cp); 4.41 (d, 1H, H<sup>1/3</sup>); 1.04 (s, 18H, CH<sub>3</sub>).

(31) *International Tables for Crystallography*; Wilson, A. J. C., Ed.; Kluwer Academic: Dordrecht, The Netherlands, 1992; Vol. C, Tables 6.1.1.4 (pp 500–502), 4.2.6.8 (pp 219–222), and 4.2.4.2 (pp 193–199).

(32) Artus, G.; Scherer, W.; Priemeier, T.; Herdtweck, E. STRUX-V, A Program System to Handle X-ray Data; TU München, München, Germany, 1997.

(33) Spek, A. L. PLATON-92 – PLUTON-92, An Integrated Tool for the Analysis of the Results of a Single-Crystal Structure Determination. *Acta Crystallogr., Sect. A* **1990**, *46*, C34.

(34) Altomare, A.; Cascarano, G.; Giacovazzo, C.; Guagliardi, A.; Burla, M. C.; Polidori, G.; and Camalli, M. SIR-92, University of Bari, Bari, Italy, 1992.

(35) Sheldrick, G. M. SHELXL-93. In *Crystallographic Computing 3*; Sheldrick, G. M., Krüger, C., Goddard, R., Eds.; Oxford University Press: Oxford, England, 1993; pp 175–189.

(36) IPDS Operating System Version 2.8; Stoe & Cie GmbH, Darmstadt, Germany, 1997.

(37) Otwinowski, Z.; Minor, W. Processing of X-ray Diffraction Data Collected in Oscillation Mode. In *Methods in Enzymology*; Carter, W. C., Sweet, R. M., Jr., Eds.; Academic Press: New York, 1996; Vol. 276.

(38) Honan, M. B.; Atwood, J. L.; Bernal, I.; Herrmann, W. A. *J. Organomet. Chem.* **1979**, *179*, 403.

**X-ray Crystallography.** Suitable single crystals for the X-ray diffraction studies were grown by standard techniques from saturated solutions of **1** in NCCH<sub>3</sub>/Et<sub>2</sub>O and of **13** in *n*-pentane/*n*-hexane/(CH<sub>3</sub>)<sub>2</sub>O/Et<sub>2</sub>O at room temperature. Both structures were solved by a combination of direct methods, difference Fourier syntheses and refined by full-matrix least-squares method. Neutral atom scattering factors for all atoms and anomalous dispersion corrections for the non-hydrogen atoms were taken from ref 31. All calculations were performed on a DEC 3000 AXP workstation with the STRUX-V<sup>32</sup> system, including the programs PLATON-92,<sup>33</sup> PLUTON-92,<sup>33</sup> SIR-92,<sup>34</sup> and SHELXL-93.<sup>35</sup>

**Data Collection, Structure Solution, and Refinement for the Complex 1.** A summary of the crystal and experimental data is reported in Table 4. Preliminary examination and data collection were carried out on an imaging plate diffraction system (IPDS; Stoe & Cie) equipped with a rotating anode (Nonius FR591; 50 kV; 60 mA; 3.0 kW) and graphite-monochromated Mo K $\alpha$  radiation. Data collection were performed at 193 K within the  $\theta$  range of 2.32° <  $\theta$  < 27.75° with an exposure time of 1.50 min per image (rotation scan modulus from  $\varphi$  = 0.0 to 180° with  $\Delta\varphi$  = 1°). A total number of 36 740 reflections were collected; 664 systematic absent reflections were rejected from the original data set. After merging, a total of 9536 independent reflections remained and were used for all calculations. Data were corrected for Lorentz and polarization effects. Corrections for absorption and decay effects were applied with the program DECAY.<sup>36</sup> The unit cell parameters were obtained by full-matrix least-squares refinements of 4551 reflections with the program CELL.<sup>36</sup> All “heavy atoms” of the asymmetric unit were anisotropically refined. Hydrogen atoms were calculated in ideal positions (riding model) and included in the structure factor calculations but not refined. Full-matrix least-squares refinements were carried out by minimizing  $\sum w(F_o^2 - F_c^2)^2$  with the SHELXL-93 weighting scheme and stopped at shift/error < 0.001.

**Data Collection, Structure Solution, and Refinement for the Complex 13.** A summary of the crystal and experimental data is reported in Table 4. Preliminary examination and data collection were carried out on a Kappa CCD area detecting diffraction system (NONIUS KCCD) equipped with a rotating anode (Nonius FR591; 50 kV; 60 mA; 3.0 kW) and graphite-monochromated Mo K $\alpha$  radiation. Data collection were performed at 173 K within the  $\theta$  range of 2.18° <  $\theta$  < 31.35° with an exposure time of 1.0 min per frame ( $\theta$  offset 10°,  $\varphi$ -start 0.0°,  $\varphi$ -end 360°,  $\Delta\varphi$  = 1°, repetition 1). A total number of 14 111 reflections were collected. After merging, a total of 7231 independent reflections remained and were used for all calculations. Data were corrected for Lorentz and polarization effects. The unit cell parameters were obtained by full-matrix least-squares refinements of 14 653 reflections. Raw data were reduced and scaled with the programs DENZO and HKL.<sup>37</sup> All “heavy atoms” of the asymmetric unit were refined anisotropically. All hydrogen atoms were found in the difference map calculated from the model containing all non-hydrogen atoms. The hydrogen positions were refined with individual isotropic displacement parameters. Full-matrix least-squares refinements were carried out by minimizing  $\sum w(F_o^2 - F_c^2)^2$  with the SHELXL-93 weighting scheme and stopped at shift/error < 0.001.

**Acknowledgment.** This work was supported by PRAXIS XXI under projects 2/2.1/QUI/316/94 and PBIC/C/QUI/220/95. C.A.G. (BD) and J.P.L. (BTL) thank PRAXIS XXI for a grant.

**Supporting Information Available:** Complete listings of data collection parameters, final fractional atomic coordinates, thermal displacement parameters, bond lengths, and bond angles for **1** and **13**. This material is available free of charge via the Internet at <http://pubs.acs.org>.